Towards Integrated Computational Materials Engineering for Quantifying Performance Impacts of Microstructure and Defect Interactions in Powder Bed Fusion Parts

Brodan Richter[1], Joshua D. Pribe[2], Samuel J.A. Hocker[1], Saikumar R. Yeratapally[3], George R. Weber[1], Vamsi R. Subraveti[4], Caglar Oskay[4], Edward H. Glaessgen[1]

[1]NASA Langley Research Center, Hampton, VA
[2]Analytical Mechanics Associates, Hampton, VA
[3]Science and Technology Corporation, Hampton, VA
[4]Vanderbilt University, Nashville, TN
brodan.m.richter@nasa.gov

International Conference on Advanced Manufacturing 2023

NTRS #20230014203

Scenario: A New Alloy was Developed

- Our group has developed a new alloy…

- What build parameters should we use?
- Should we be concerned about defects?
- How will the new material perform?
- How long will this take to qualify?

How should these questions be addressed?

Scanning velocity?
Hatch spacing?
Laser power?
Beam diameter?
Scan strategy?
Contouring parameters?
Location in chamber?
Rotation angle?
Orientation of part?
Plate temperature?
Layer thickness?
And more…

Scenario: A New Alloy was Developed

- Use heuristics?
  - Select parameters based on alloys with similar properties?
  - Reasonable, but need prior knowledge.
  - Also, which properties are the most important?
  - Thermophysical, absorptivity, powder, phases…

- Conduct an experimental survey?
- +11 parameters, 2 levels each…
  - 2048 samples. Can down-select parameters, but still may need multiple rounds of printing

For both, still need to…

- Cross-section, polish, etch, and examine the samples
- Execute x-ray computed tomography scans
- Perform tensile tests, fatigue tests….

Costs add up fast

Computational Process-Structure-Property (PSP) models provide a way to augment these approaches

PSP Models: Our Approach

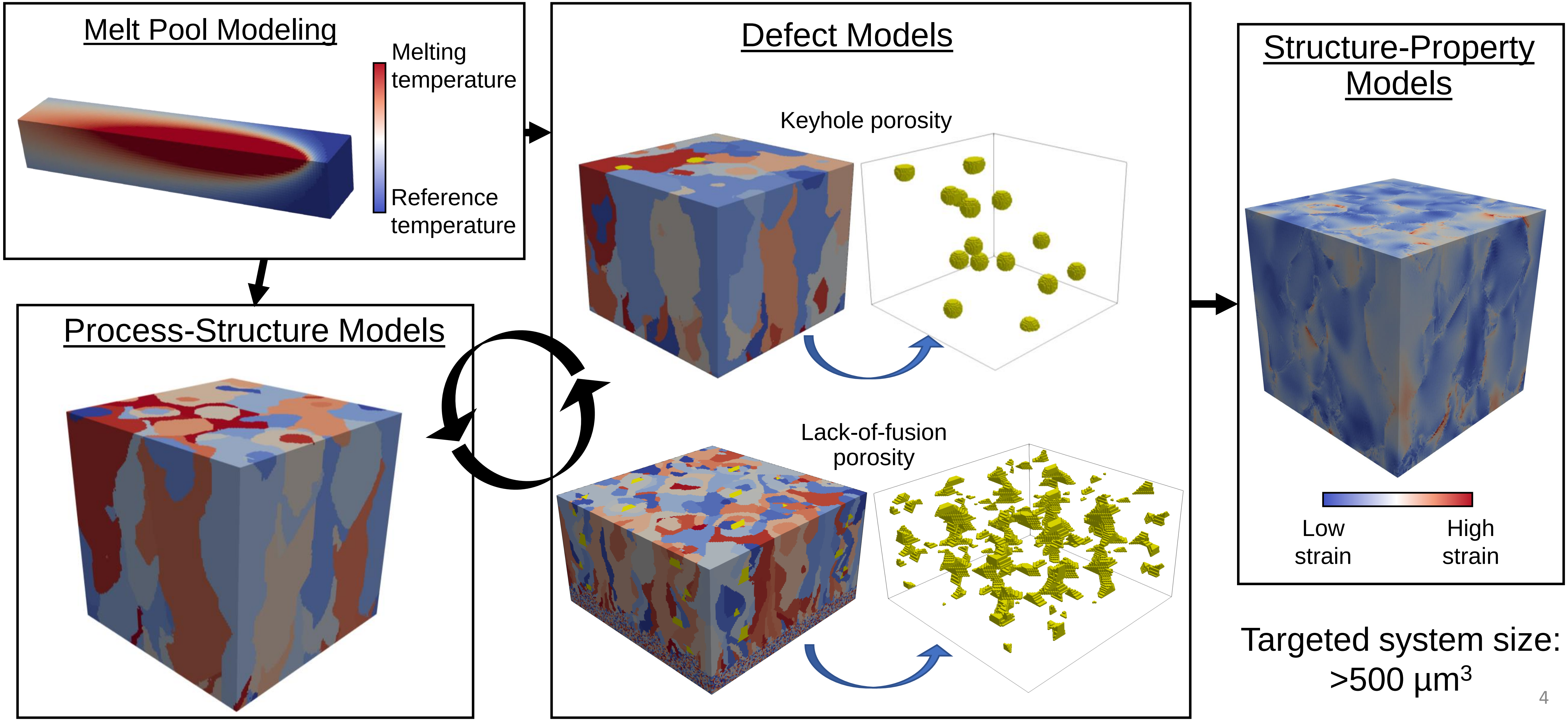

Targeted system size:
>500 μm^3

PSP Models: Process-Structure Models

Melt Pool Modeling

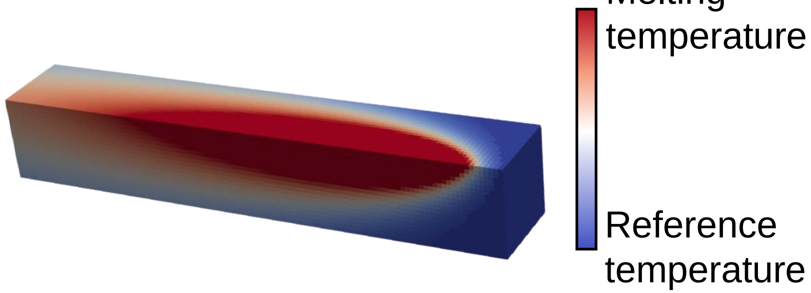

Process-Structure Models

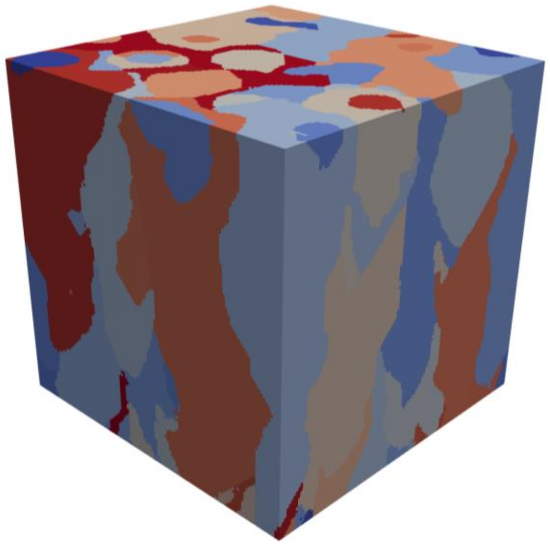

Defect Models

Keyhole porosity

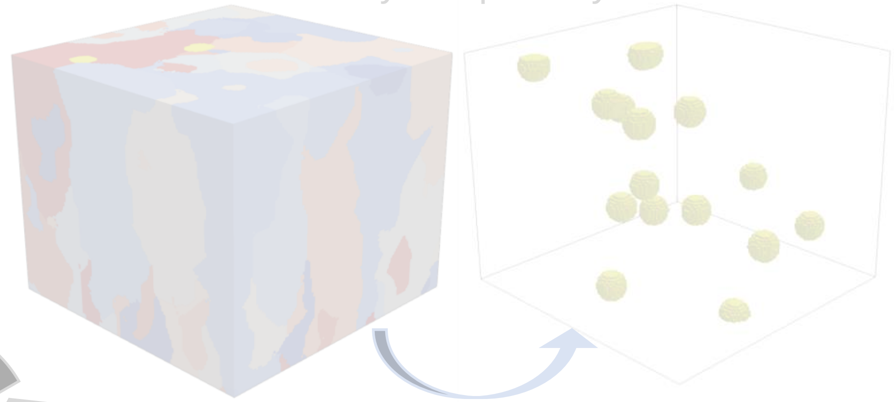

Lack-of-fusion
porosity

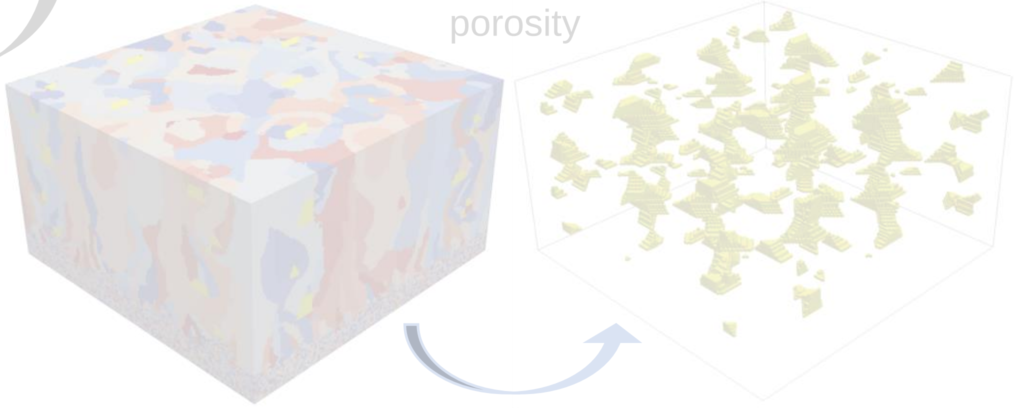

Structure-Property Models

Targeted system size:
>500 μm^3

Physically-based Monte Carlo Modeling

- **S**tochastic **P**arallel **Par**ticle **K**inetic **S**imulator (SPPARKS)*
  - Kinetic Monte Carlo framework from Sandia National Laboratories https://spparks.github.io/
  - Initially used for bulk microstructural evolution (e.g., annealing, recrystallization)
- Application to AM: Physically-based Monte Carlo [1,2]
  - Thermal model → temperature field → melt pool

Melt pool from analytical thermal model (Rosenthal equation)

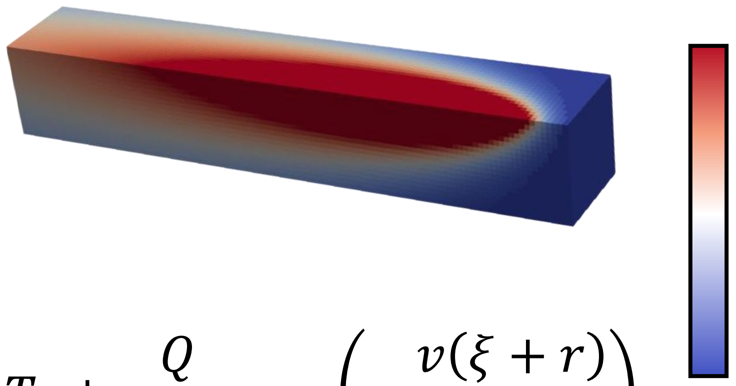

$$T = T_0 + \frac{Q}{2\pi r k} \exp\left(-\frac{v(\xi + r)}{2\alpha}\right)$$

Where:

T: temperature
T_0: background temperature
Q: absorbed power
v: scan speed
k: thermal conductivity
$\alpha = k/(\rho c_p)$
ρ: mass density
c_p: specific heat capacity
$r = \sqrt{\xi^2 + y^2 + (\eta_z z)^2}$
ξ, y, z: local coordinates
η_z: scale factor to control melt pool depth

[1] T.M. Rodgers et al., 2021
[2] J.G. Pauza et al., 2021

*The use of specific software names does not imply an endorsement by the U.S. Government or NASA.

Physically-based Monte Carlo Modeling

- **S**tochastic **P**arallel **Par**ticle **K**inetic **S**imulator (SPPARKS)*
  - Kinetic Monte Carlo framework from Sandia National Laboratories https://spparks.github.io/
  - Initially used for bulk microstructural evolution (e.g., annealing, recrystallization)
- Application to AM: Physically-based Monte Carlo [1,2]
  - Thermal model → temperature field → melt pool
  - Solidification → epitaxial grain growth

Melt pool from analytical thermal model (Rosenthal equation)

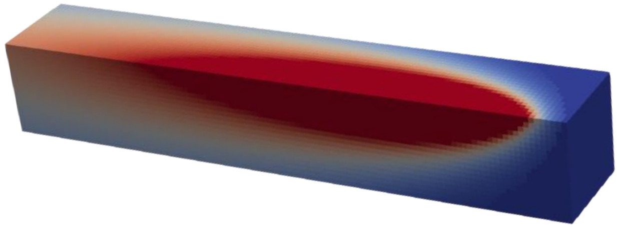

Scan strategy (schematic)

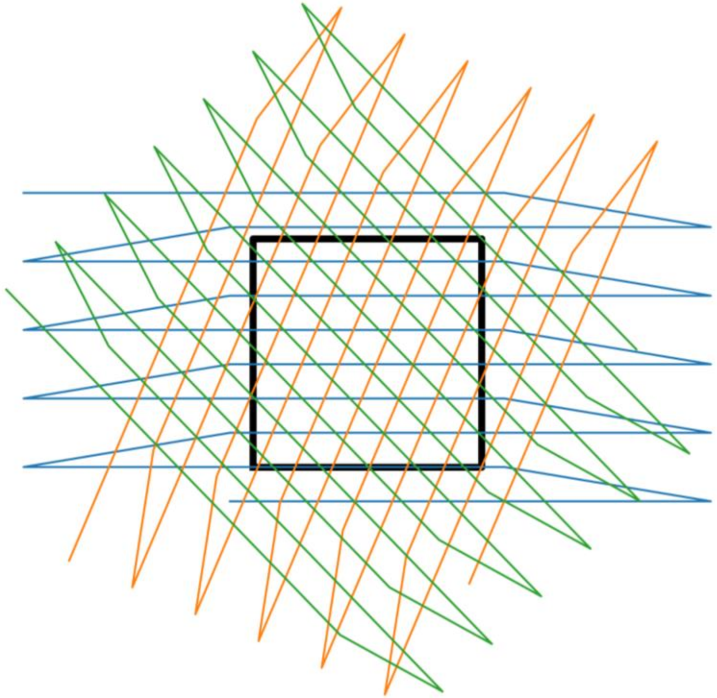

Example microstructure

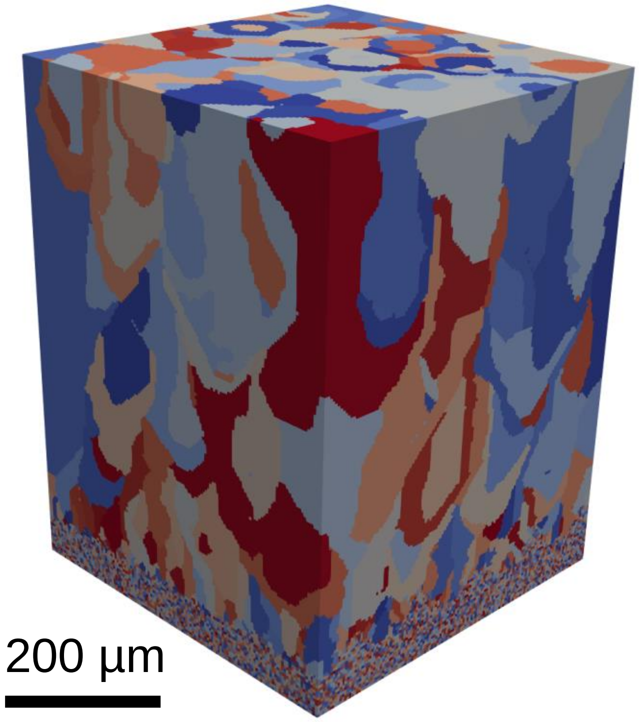

[1] T.M. Rodgers et al., 2021
[2] J.G. Pauza et al., 2021

*The use of specific software names does not imply an endorsement by the U.S. Government or NASA.

Physically-based Monte Carlo Modeling

Solidification: select probabilistically from eligible grains*

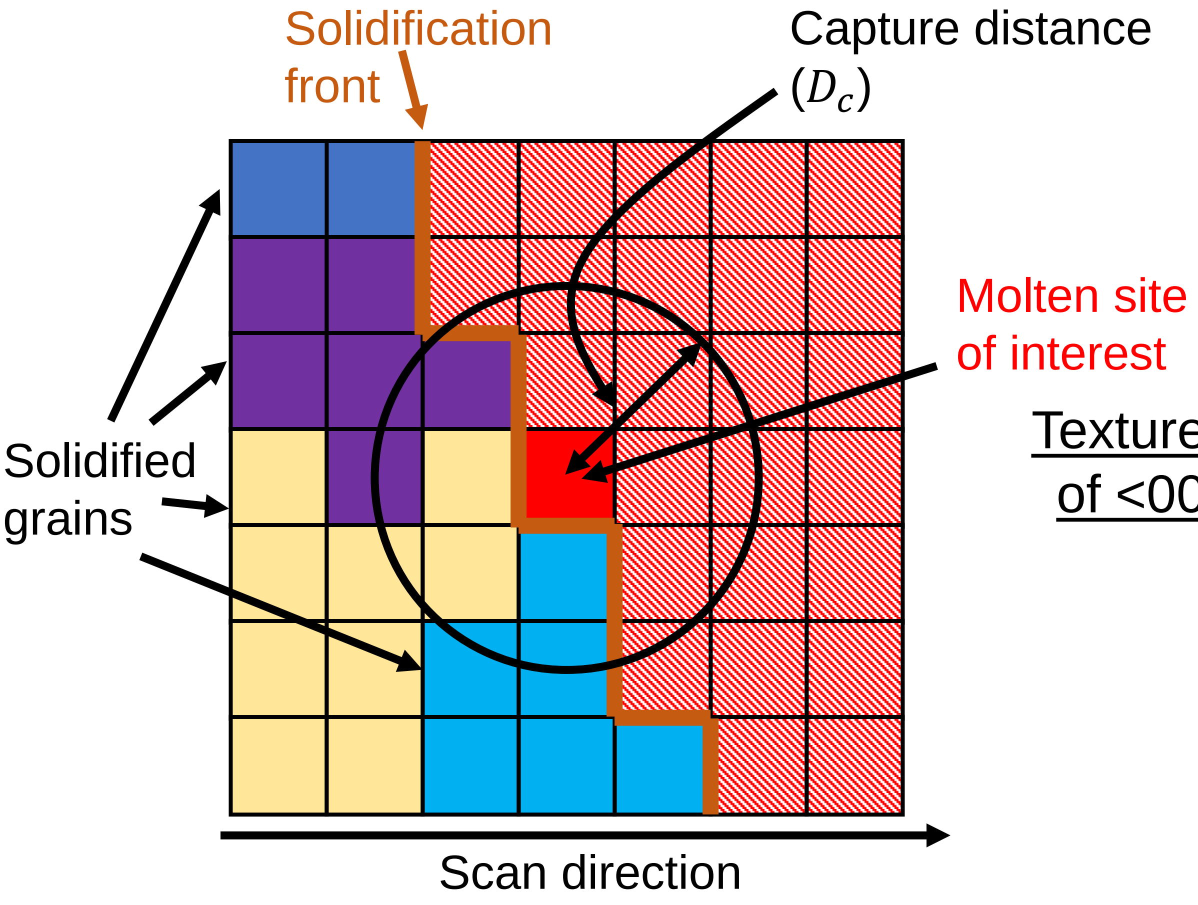

Capture distance is related to local undercooling and dendrite interface kinetics

$$D_c = \sum_{T<T_l} V(T)dt$$

$$V(\Delta T) = a\Delta T^b$$

dt: time step

Texture develops by weighing (W_i) based on alignment of <001> crystal directions with temperature gradient

$$D_{c,grain\ i} = W_i \sum_{T<T_l} V(T)dt$$

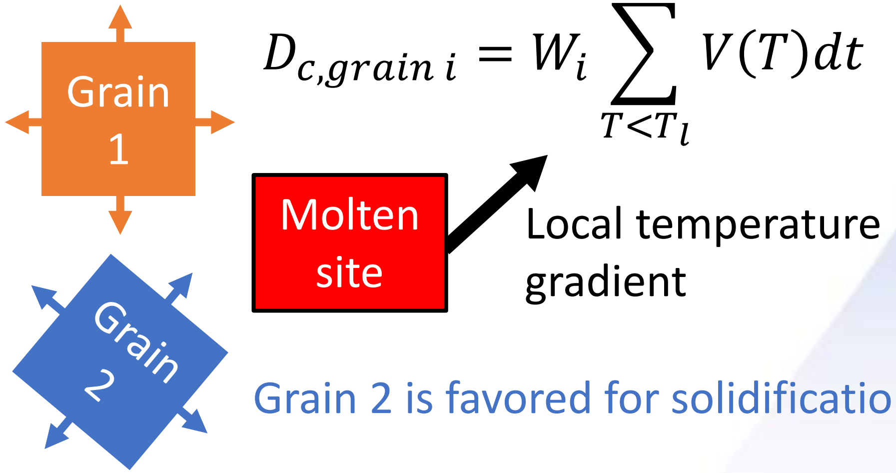

Grain 2 is favored for solidification

*Adapted from Rodgers, T.M. et al., 2021 [1]

Experimental Samples and Numerical Study

2^2 Factorial Design with Center Point (values half-way between end points)

- 600 µm x 600 µm x 695 µm numerical domain (20 layers)
- Experimentally characterized P1 and P4
- Hatch Spacing = 100 µm
- Layer Thickness = 30 µm
- Rotation between layers = 67°

Results adapted from B. Richter et al., 2022 [3]

256 µm × 512 µm X-Y Plane

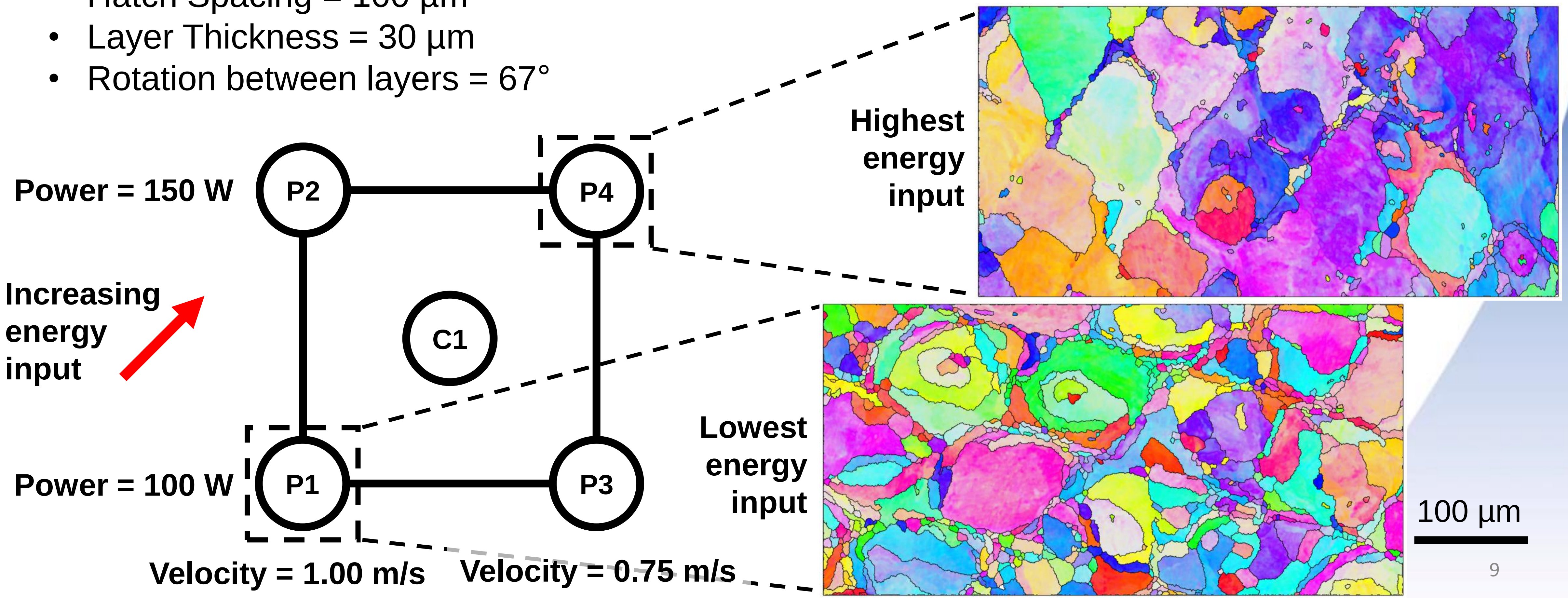

Simulated Microstructure vs. Energy Input

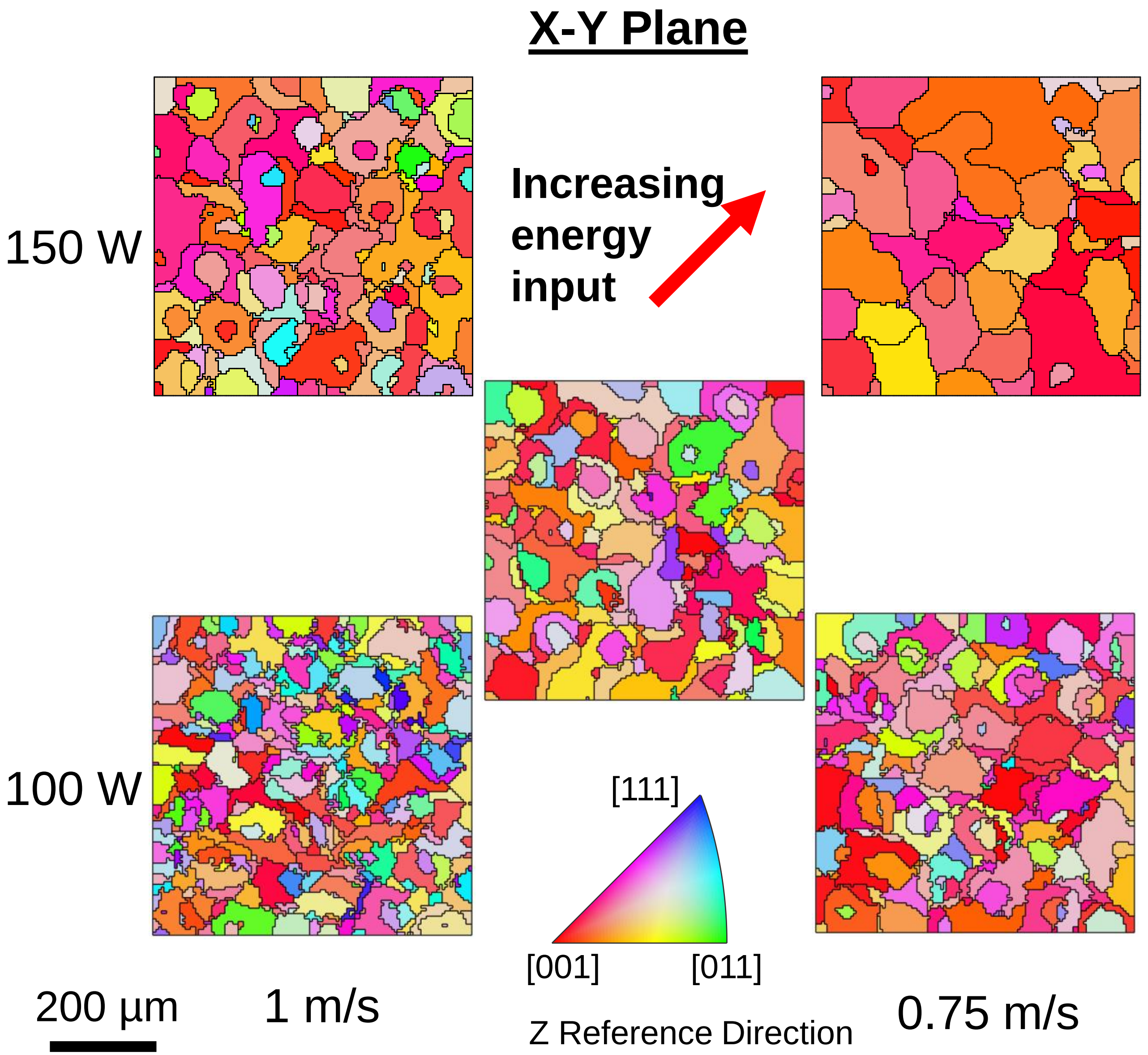

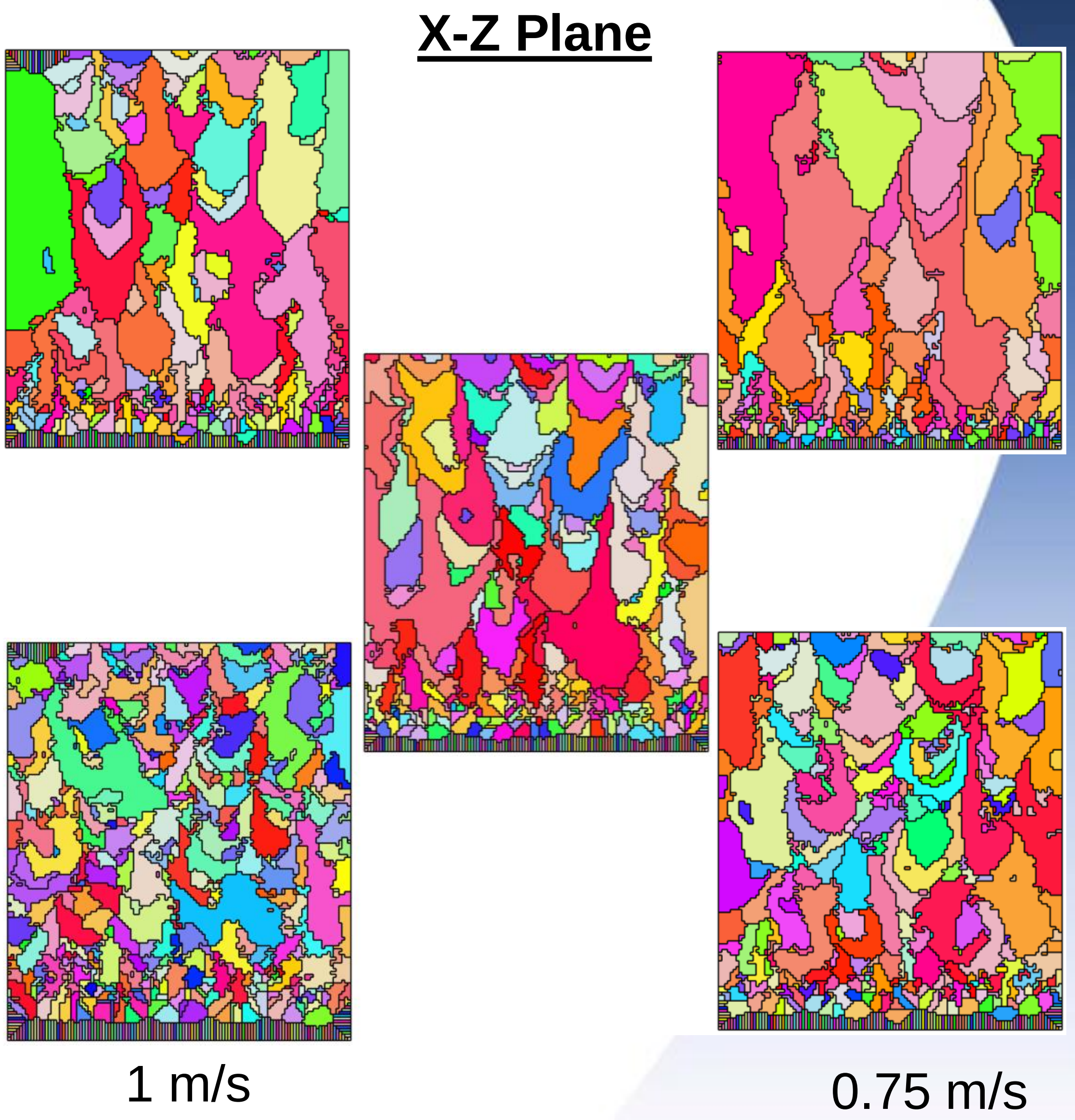

Comparison with Experiment – Low Energy

- Simulation overestimates equivalent radius approximately 17%
- Good agreement for aspect ratio (~12% difference)

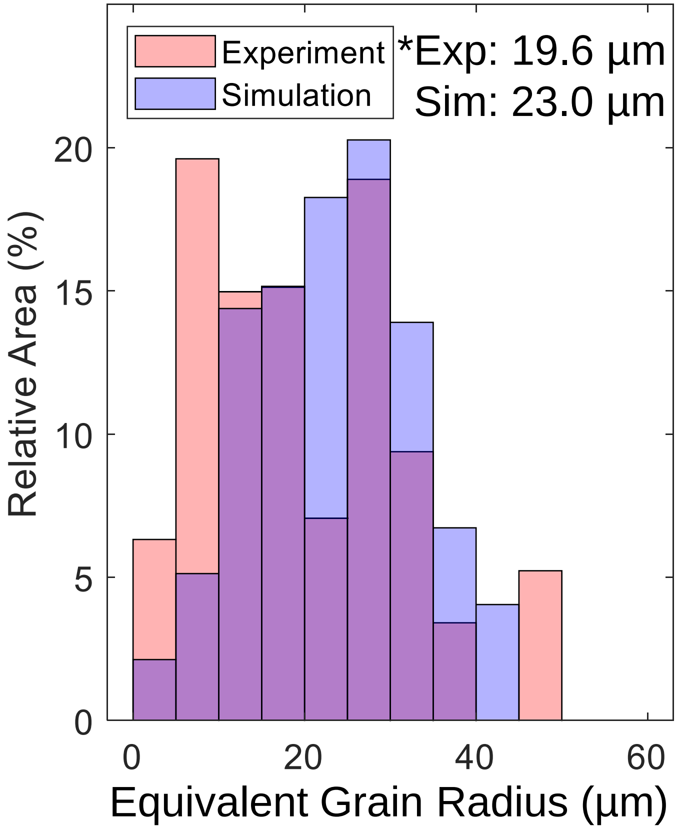

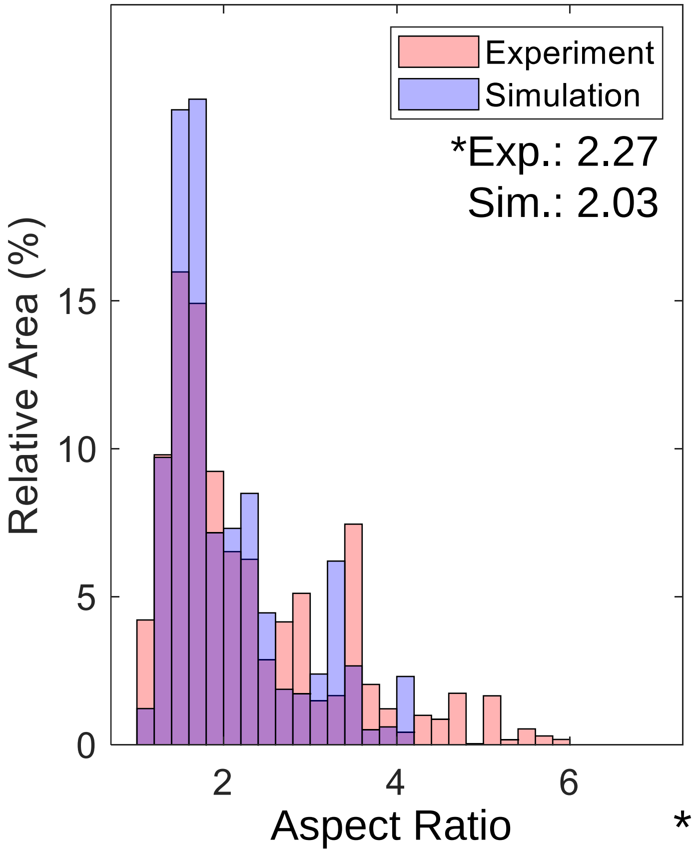

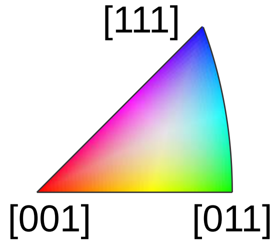

Simulation (top) and Experiment (bottom)

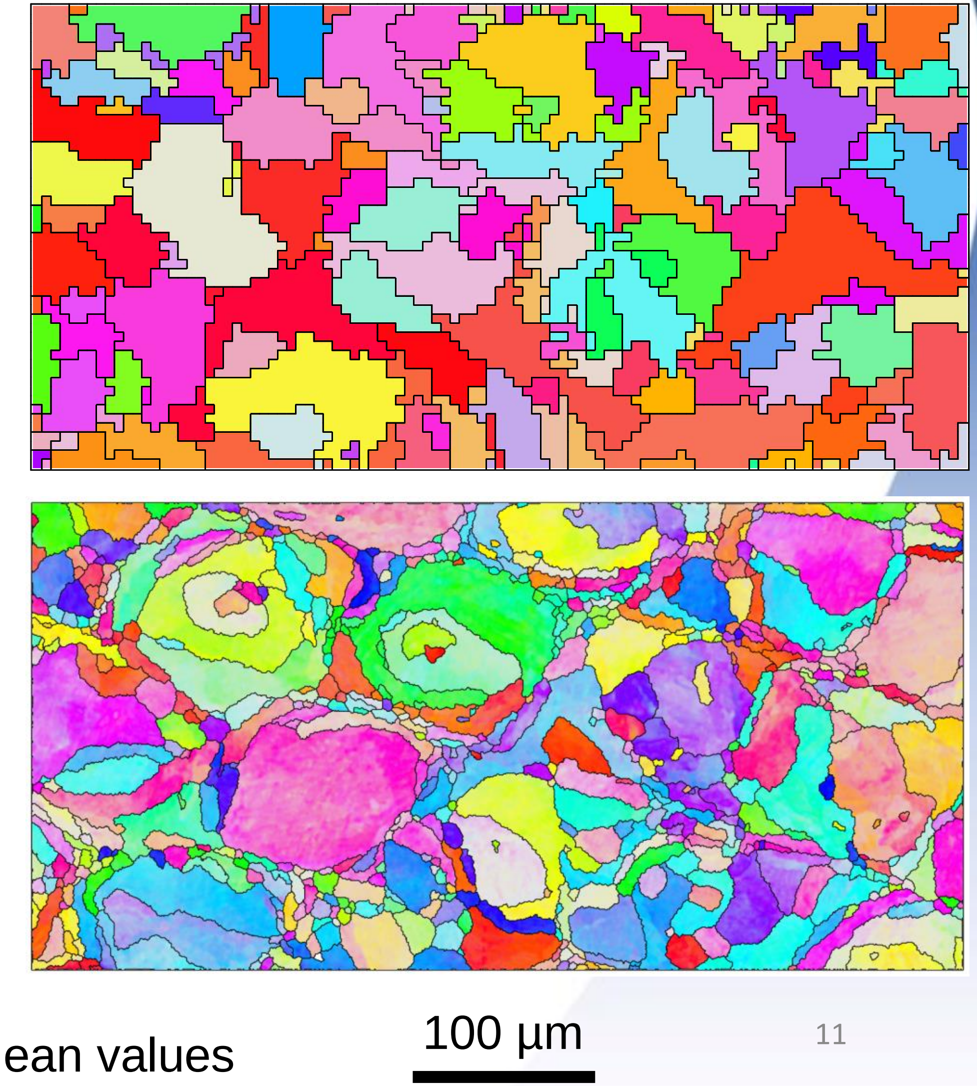

* Mean values

Comparison with Experiment – High Energy

- Simulation overestimates equivalent radius approximately 18%
- Good agreement for aspect ratio (~9% difference)

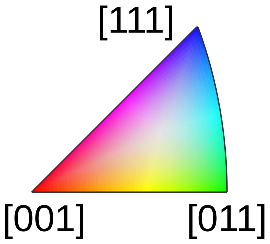

Simulation (top) and Experiment (bottom)

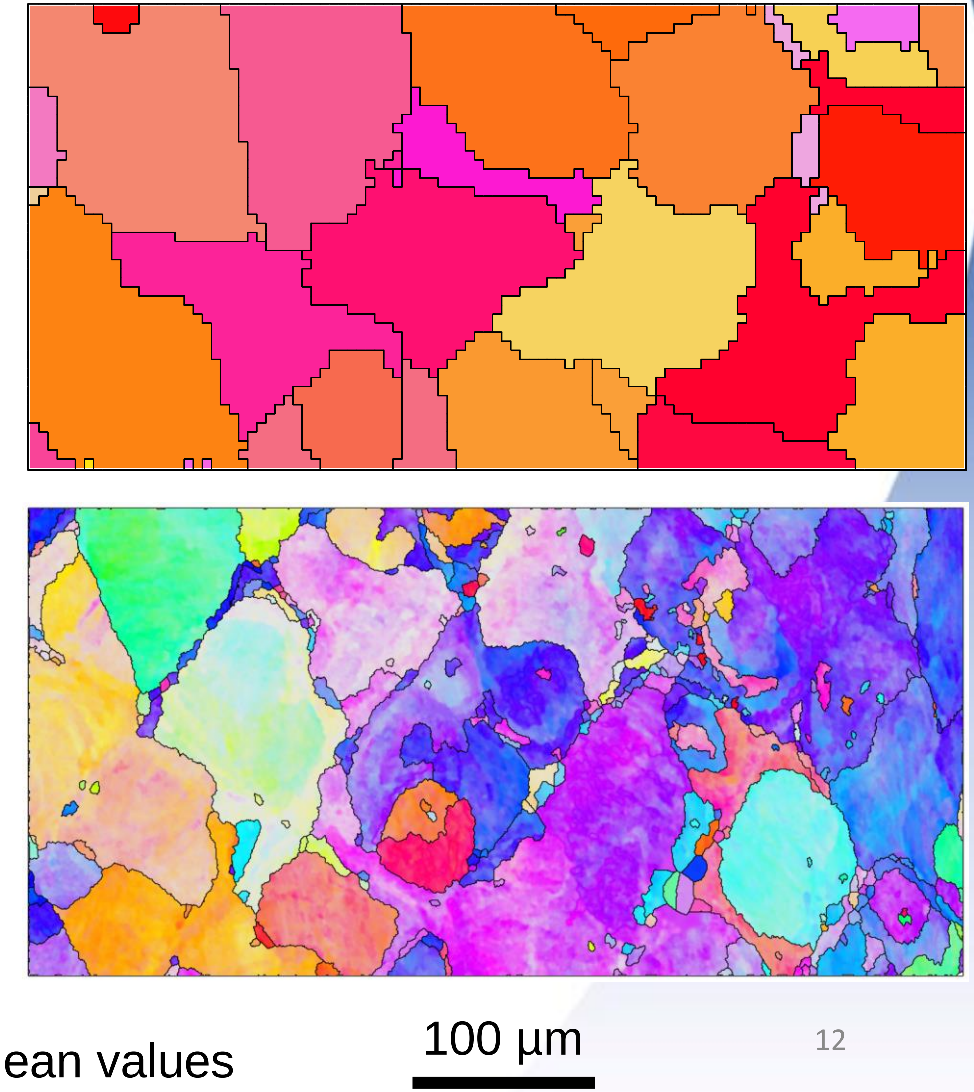

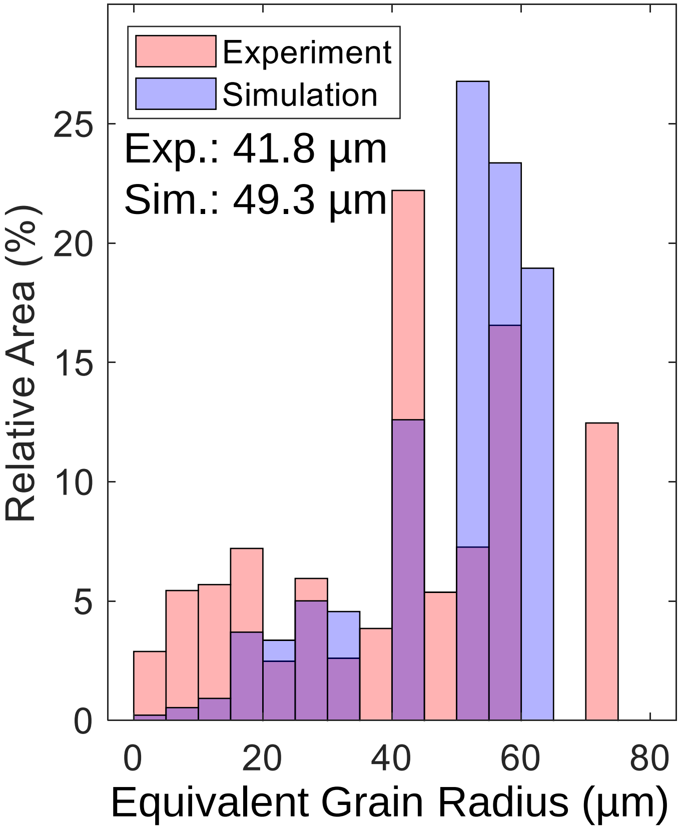

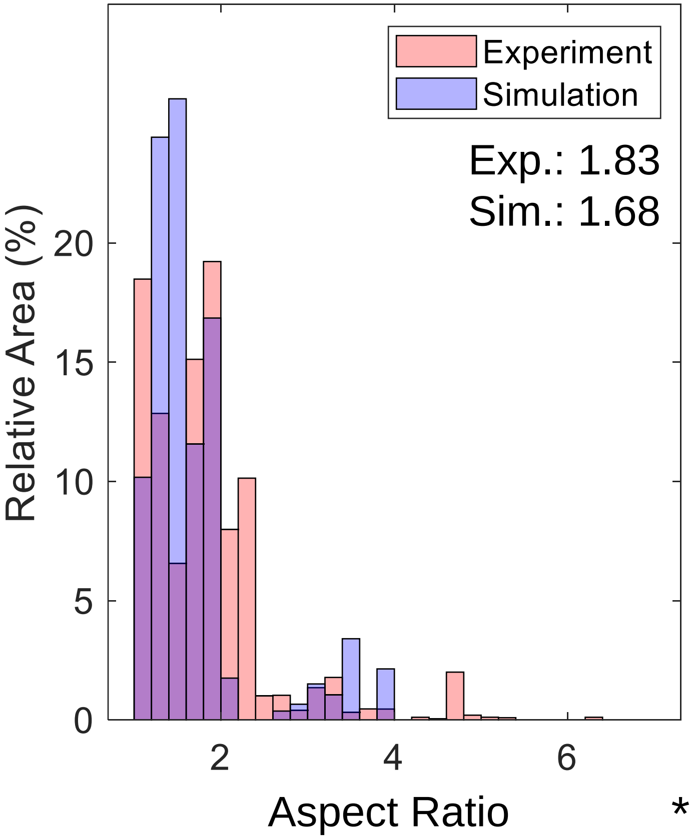

* Mean values

PSP Models: Defect Models

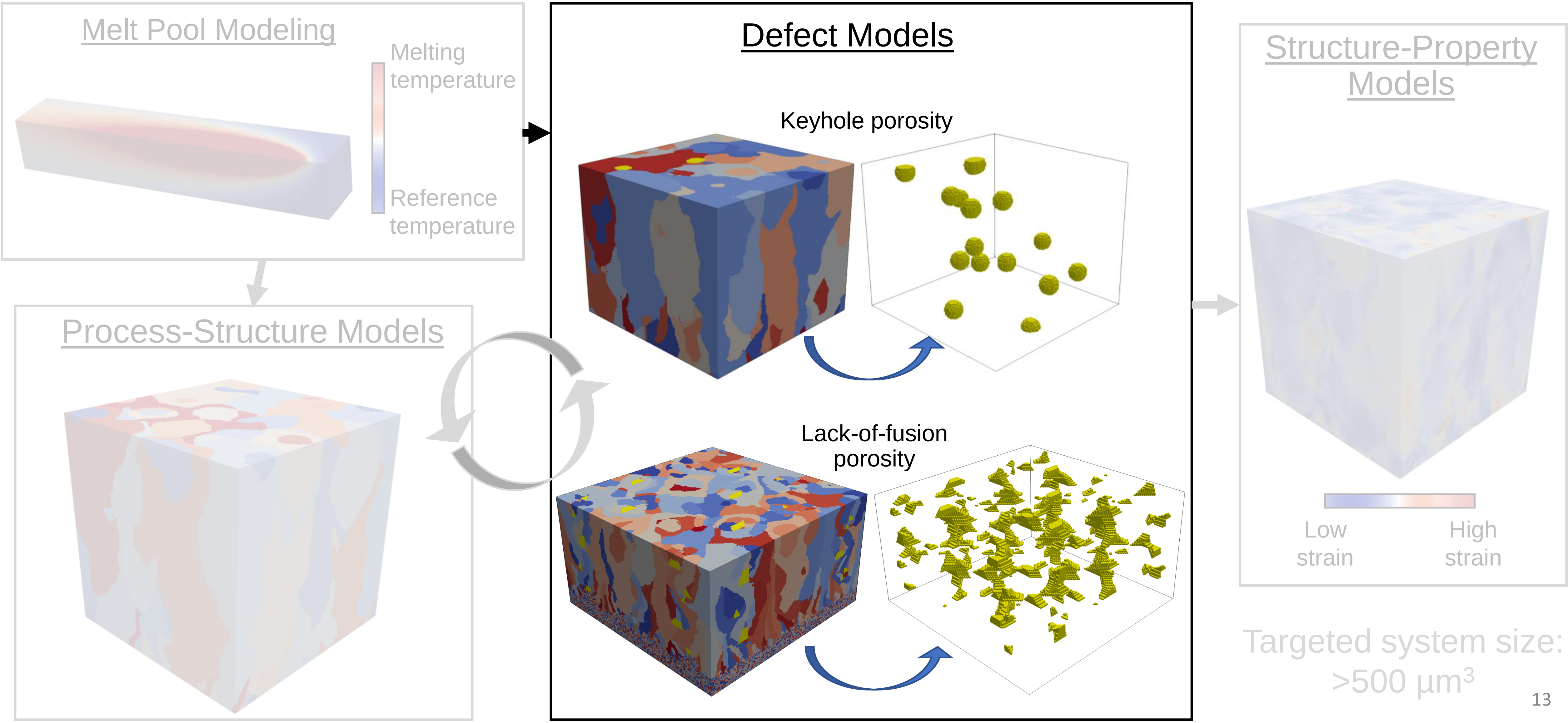

Targeted system size: >500 μm^3

PSP Models: Defect Models

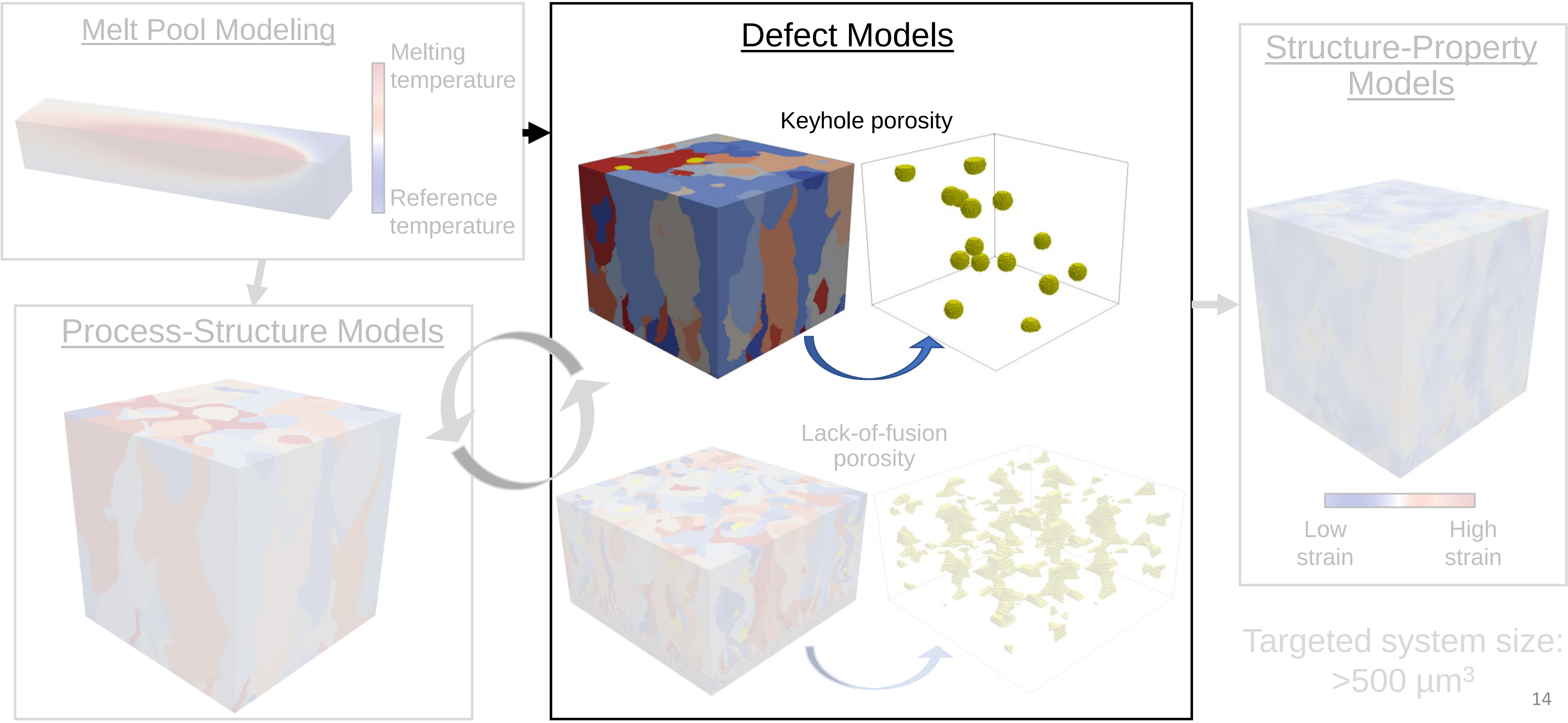

Defects Models: Keyhole Porosity

- Stochastic process
- Keyhole size and instability depends on material constant and laser parameters
- Keyhole number (Ke) used to relate keyhole behavior to processing

$$Ke = C\frac{P}{\sqrt{VR^3}}$$

C: Material constant
P: Laser power
V: Scanning velocity
R: Beam radius

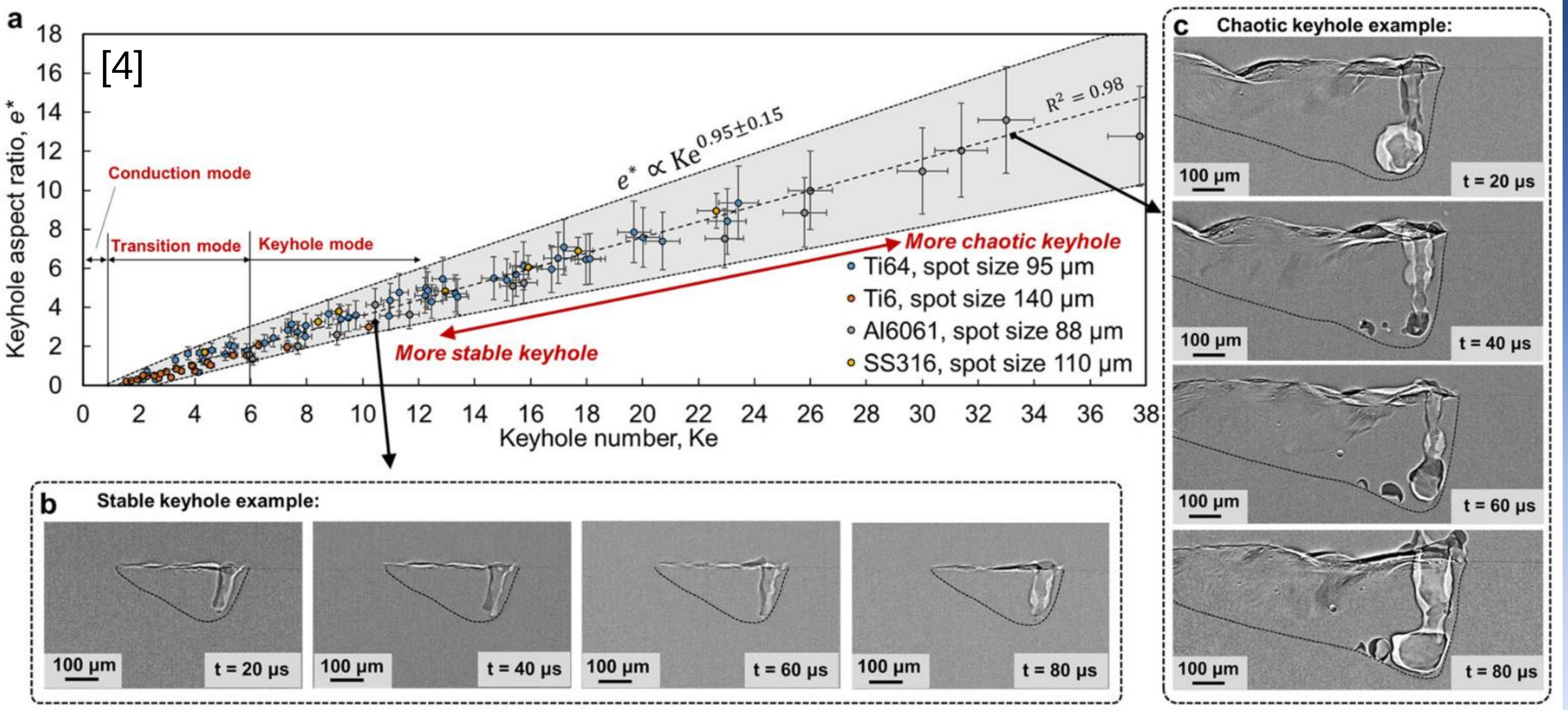

Fig. 1 One-dimensional law for keyhole aspect ratio controlled by the Keyhole number.

[4] Gan, Z. et al., 2021

Defects Models: Keyhole Porosity

- By characterizing keyhole porosity across a range of processing conditions, can fit distributions to integrate alongside computational models

Example of an experimental platen
- 2 powers (~260 W and 360 W)
- 14 velocities (0.25 m/s – 1.4 m/s)
- 5 mm lines, 6 repetitions

Purposely had many low scanning velocities and high power to induce keyhole porosity

Analyzed porosity based on individual line location

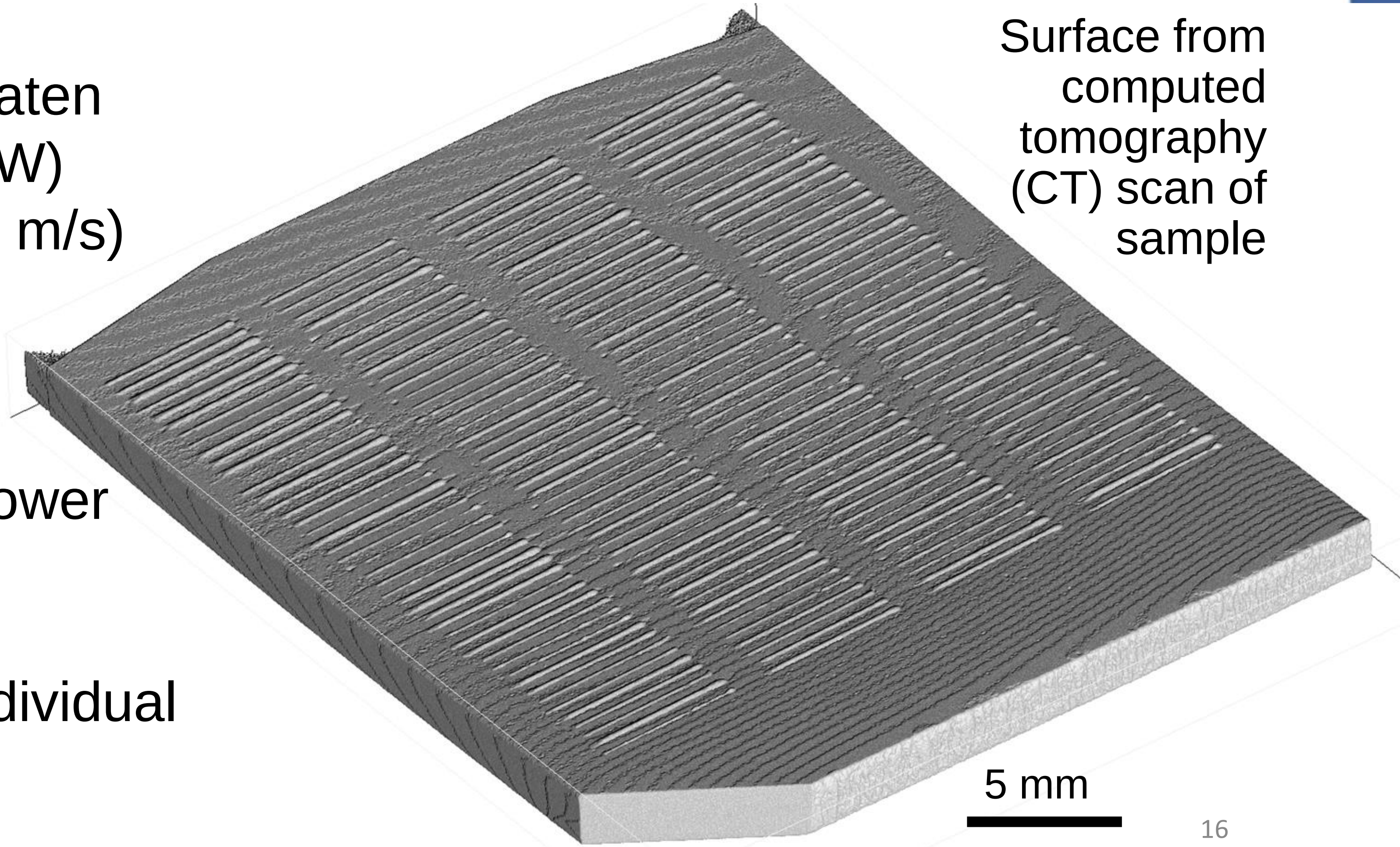

Surface from computed tomography (CT) scan of sample

Defects Models: Keyhole Porosity

CT scan of surface of sample

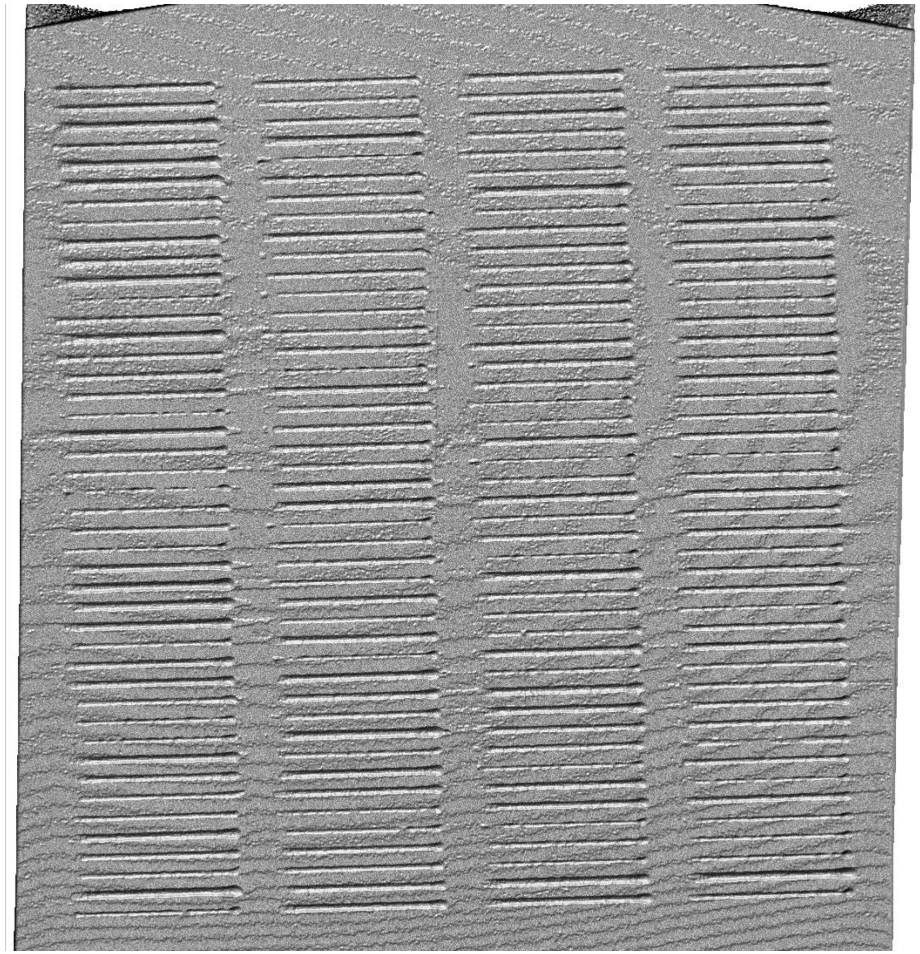

Segmented porosity

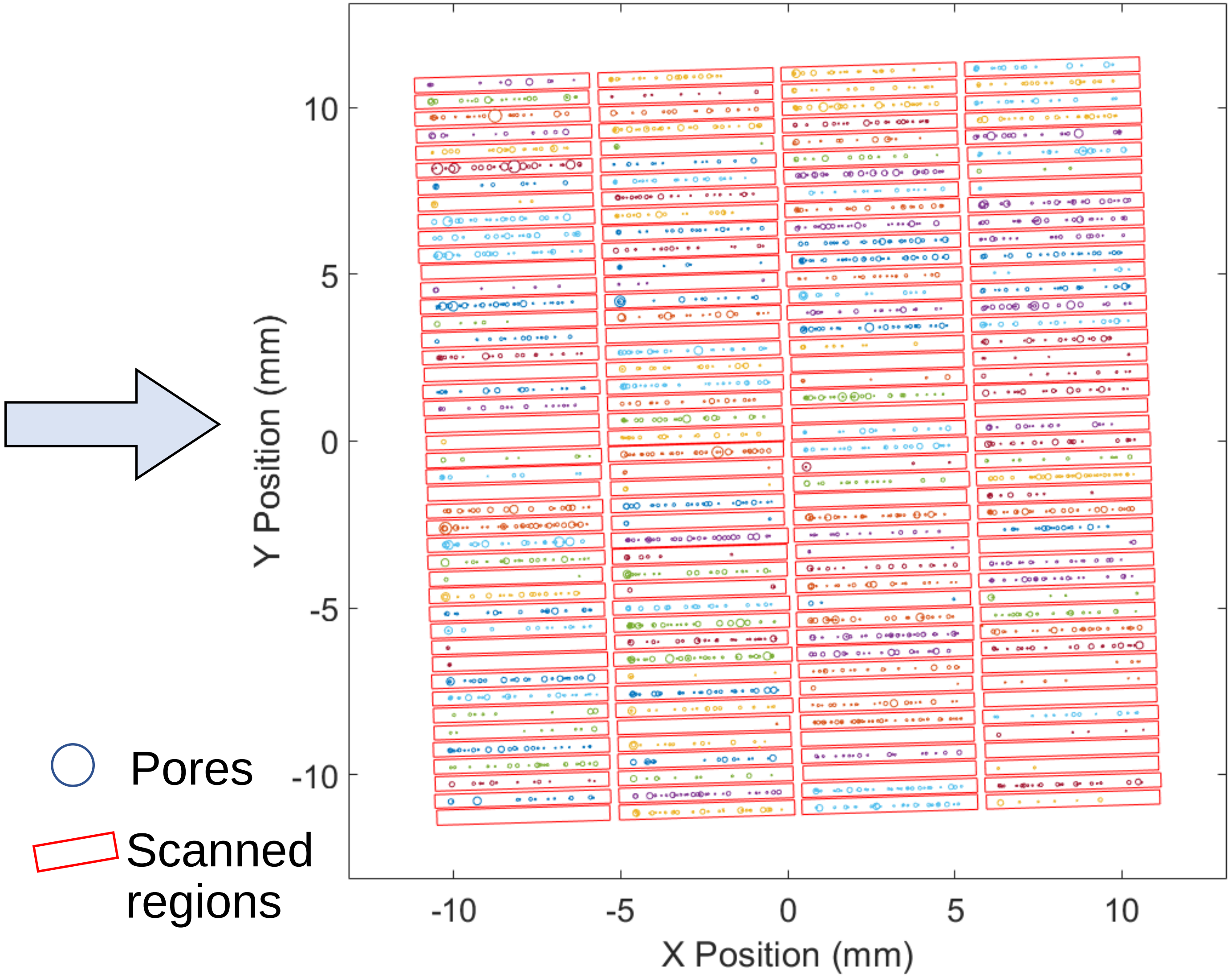

Defects Models: Keyhole Porosity

- From keyhole porosity data, can relate porosity to processing parameters

- Can sample distributions and seed into models while they're running

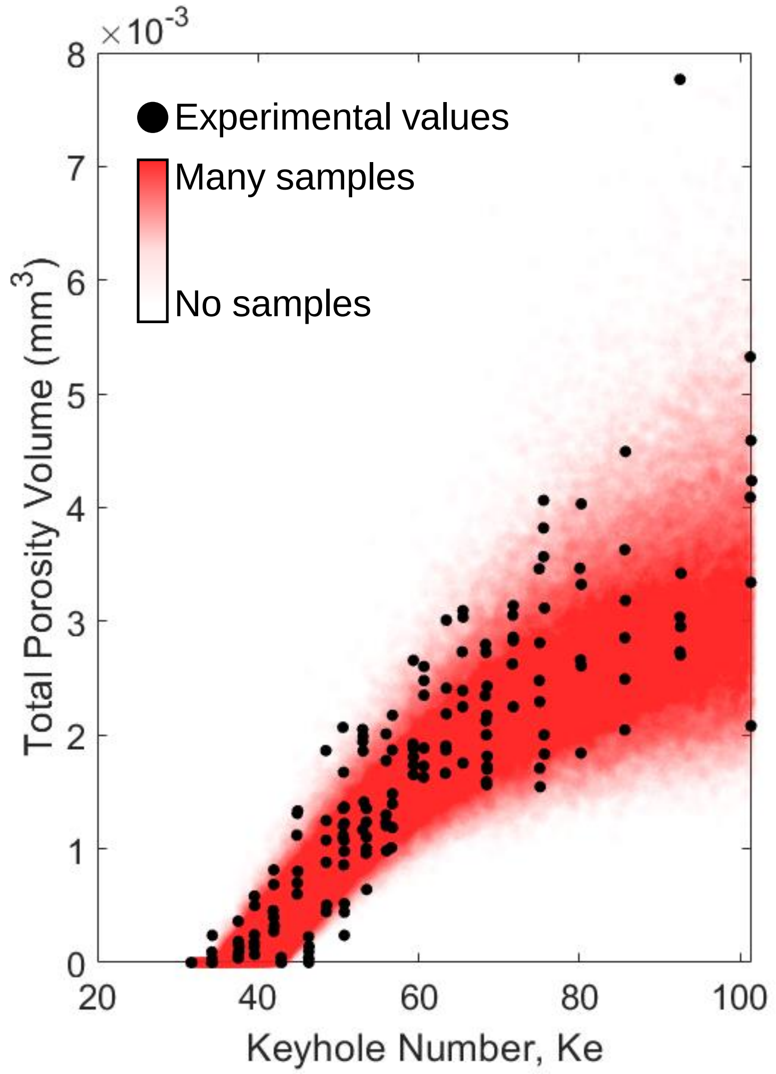

Sample pores and seed into simulation

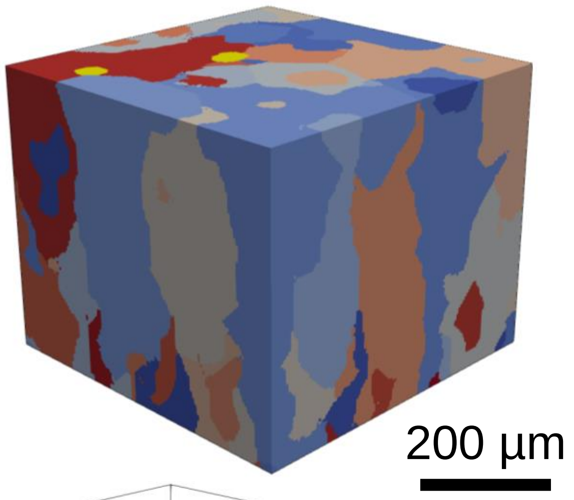

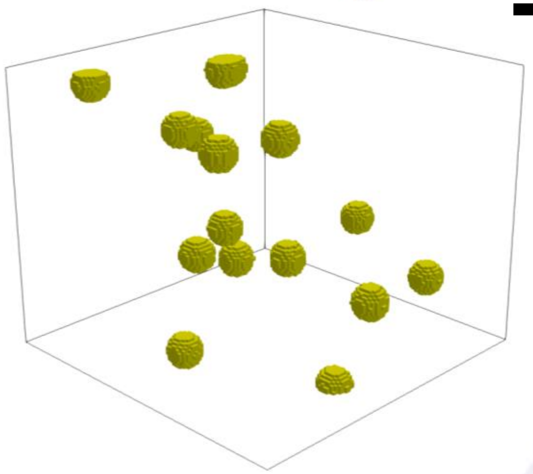

PSP Models: Defect Models

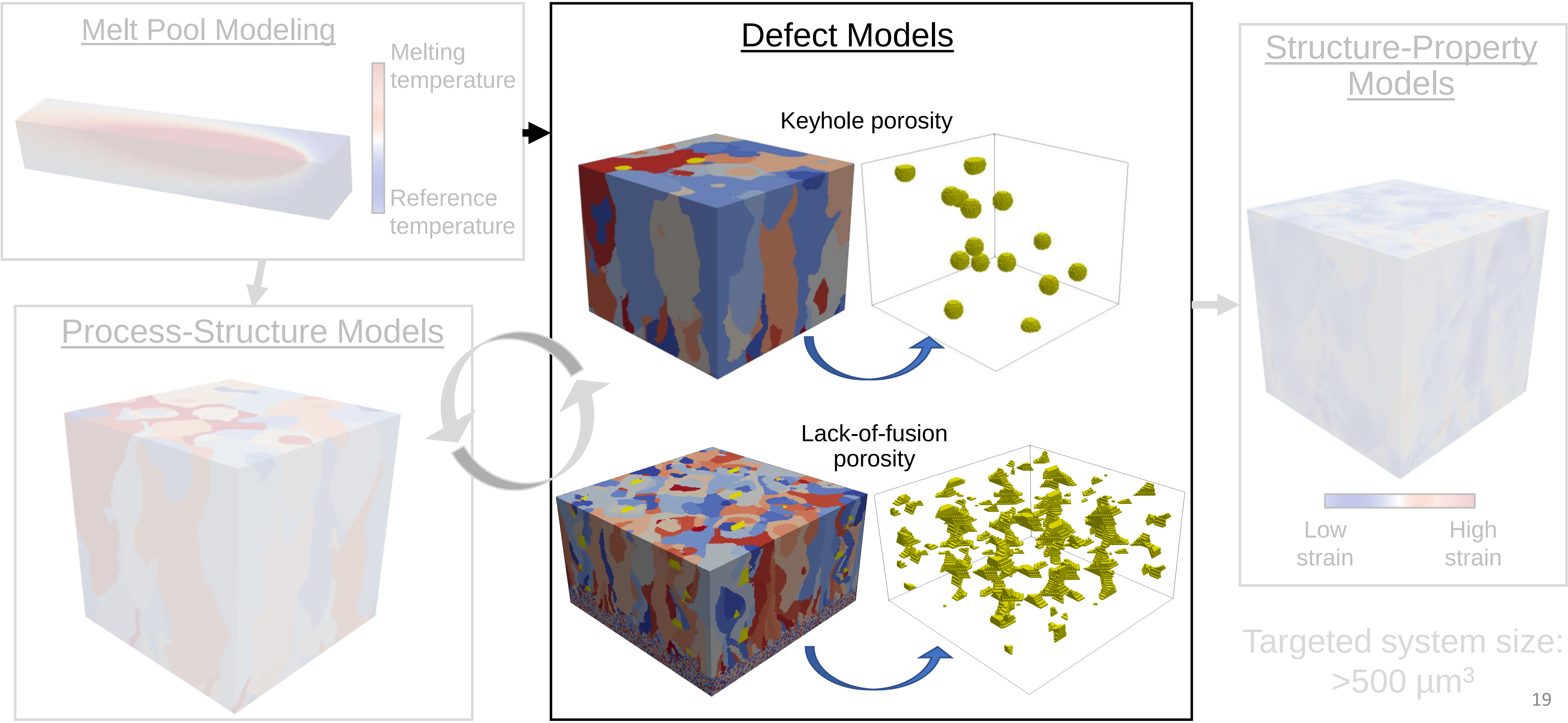

PSP Models: Defect Models

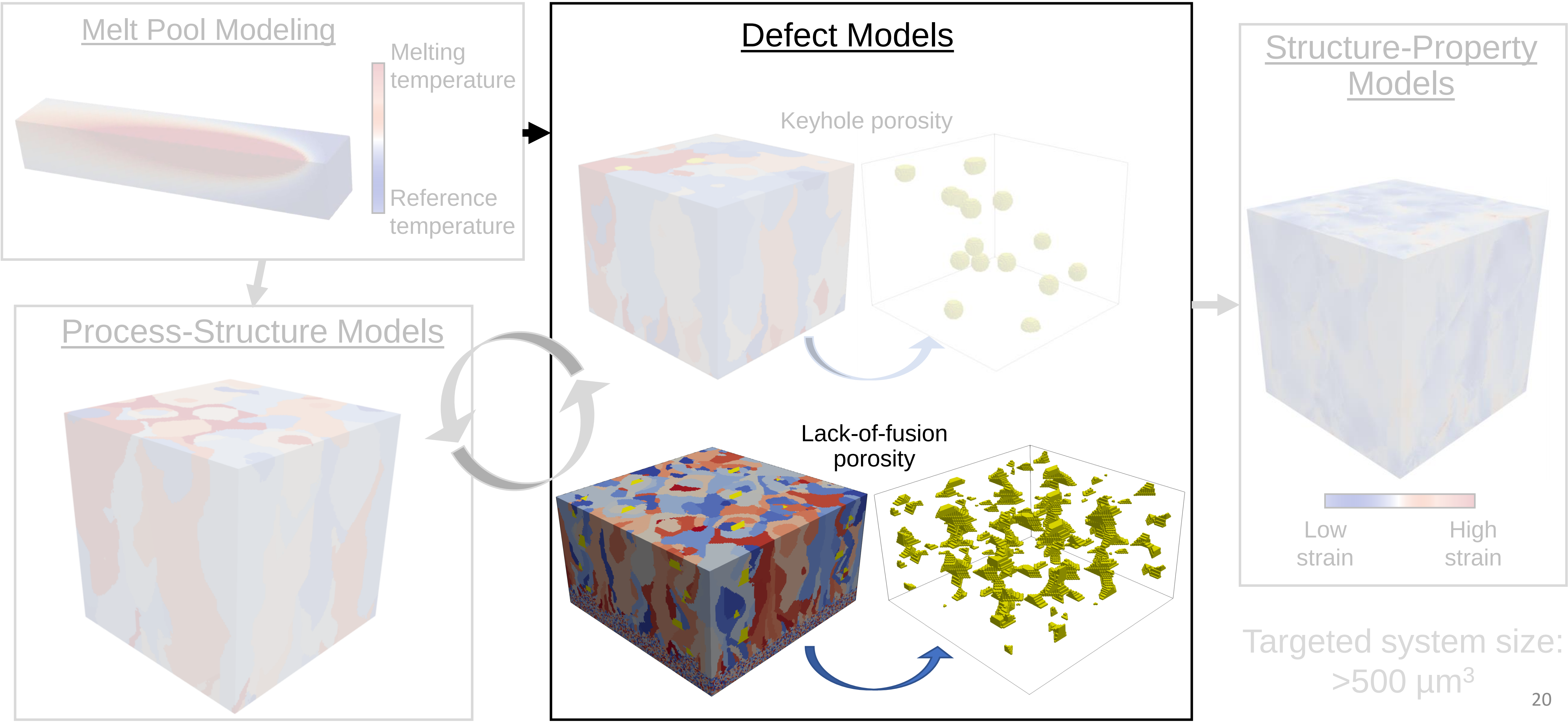

Defects Models: Lack-of-Fusion Porosity

- Lack-of-fusion porosity is semi-deterministic and geometry related
- Tang et al. derived a lack-of-fusion criteria based on the melt pool geometry and processing [5]

No porosity occurs if …

$$\left(\frac{L}{D}\right)^2 + \left(\frac{H}{W}\right)^2 \leq 1$$

L: Layer thickness
H: Hatch spacing
W: Melt pool width
D: Melt pool depth

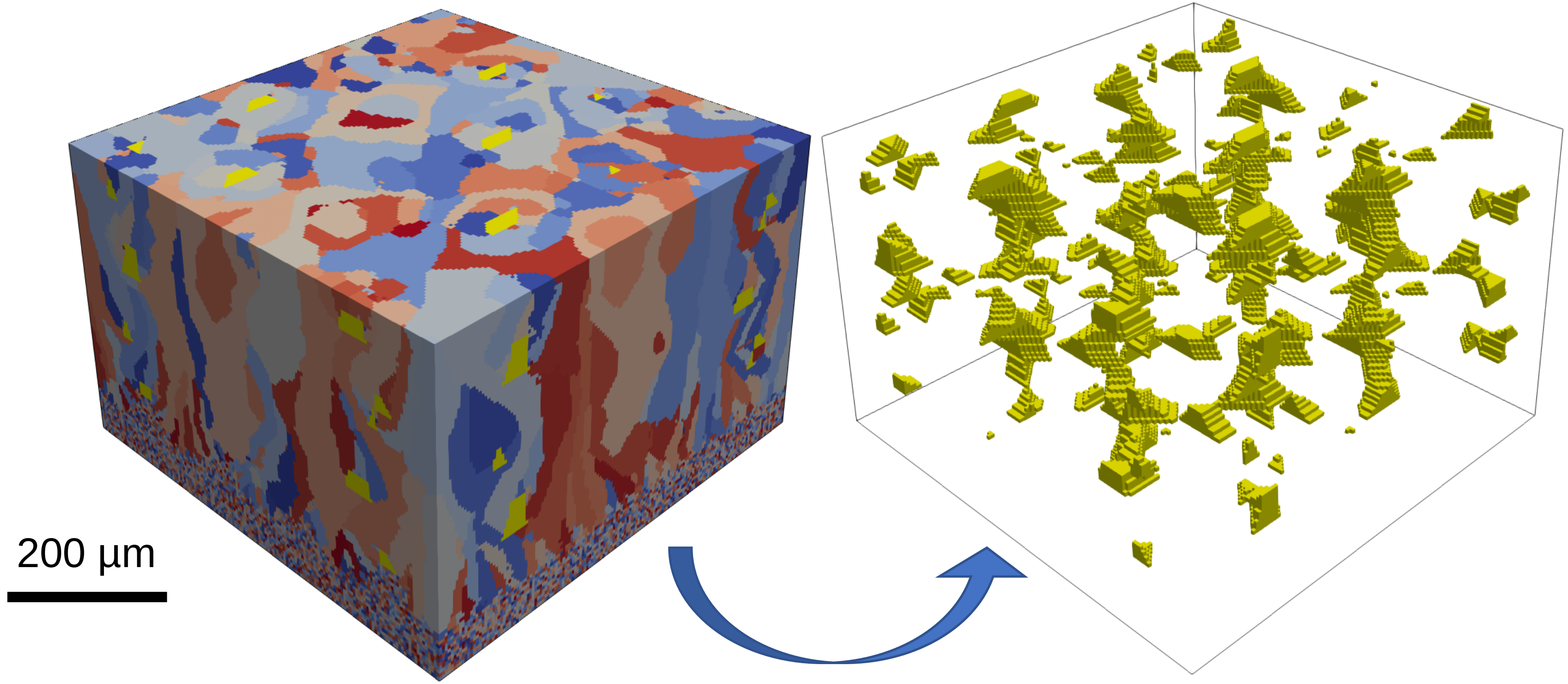

[5] M. Tang et al., 2017

Defects Models: Lack-of-Fusion Porosity

- By using a thermal model to calculate temperature field and calculating the melt pool geometry, a user can determine if porosity will occur
- If occurrence is likely, can track in process-structure model using distinct phases for melted vs. unmelted material

Melt pool from analytical thermal model (Rosenthal equation)

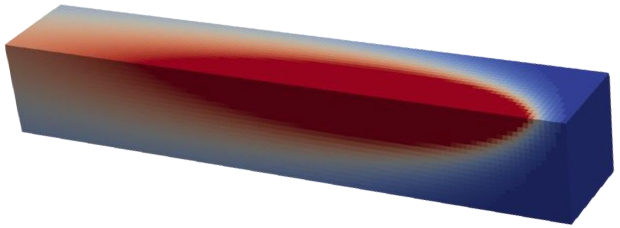

$$T = T_0 + \frac{Q}{2\pi r k} \exp\left(-\frac{v(\xi + r)}{2\alpha}\right)$$

Melt pool geometry relationship

$$W, D = f(Processing, Material)$$

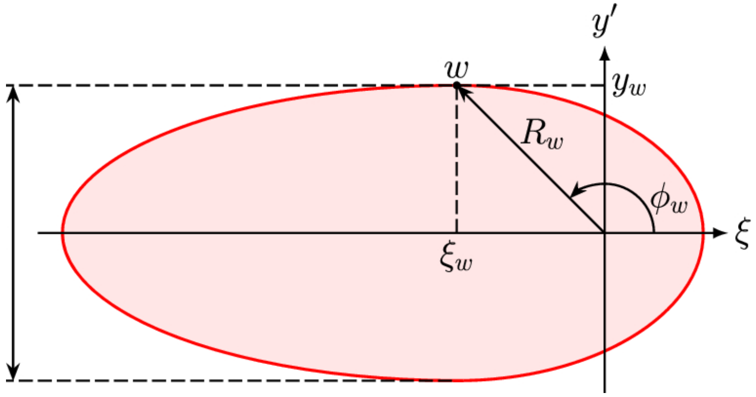

$$\left(\frac{L}{D}\right)^2 + \left(\frac{H}{W}\right)^2 \leq 1$$

Lack-of-fusion criteria

Adapted from J.D. Pribe et al., 2023 [6]

PSP Models: Structure-Property Models

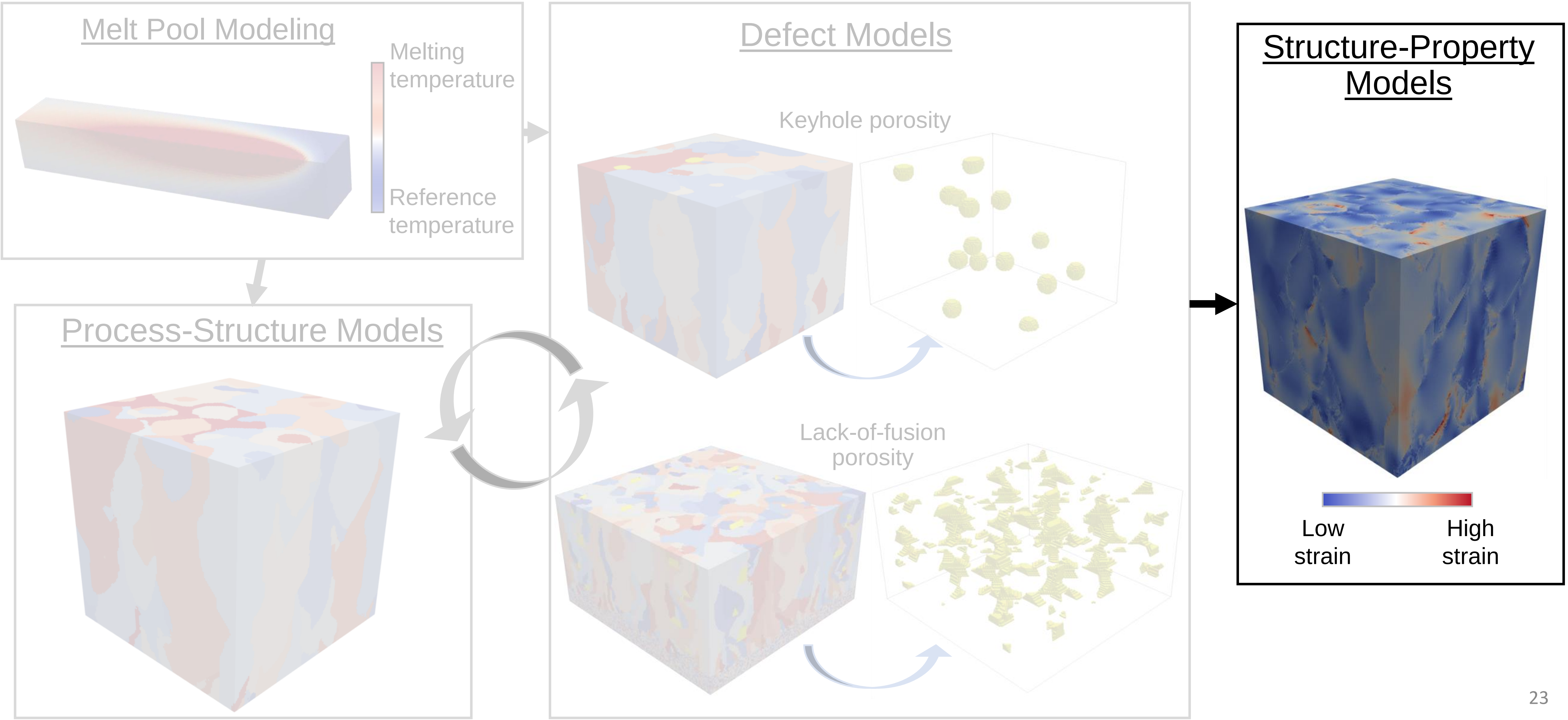

Structure-Property: Crystal Plasticity

- **E**lasto-**V**isco**p**lastic **F**ast **F**ourier **T**ransform (EVP-FFT) [7]*
- Advantages
  - Speed improvements over crystal plasticity finite element methods
  - Shares voxel-based microstructure representation with SPPARKS

Section adapted from J.D. Pribe et al., 2023 [6]

One of 12 possible α variants randomly selected for each grain

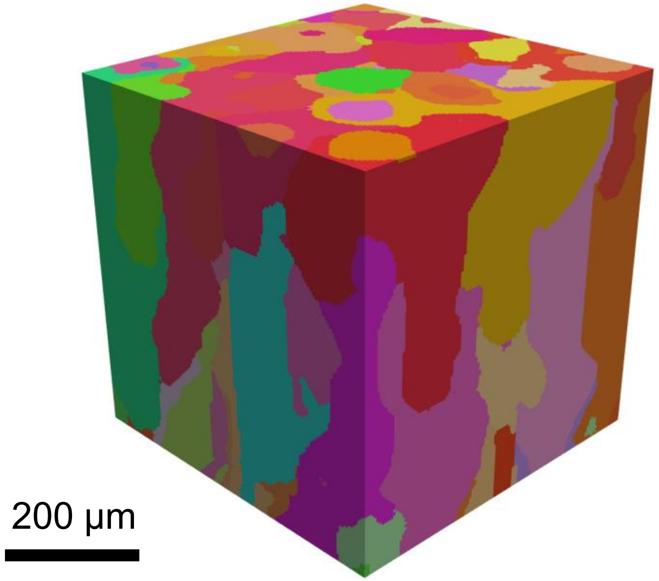

Prior β texture, *z* ref. direction

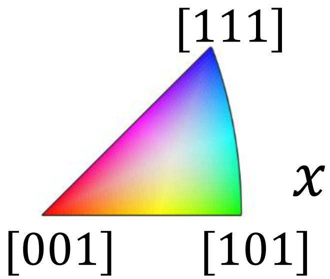

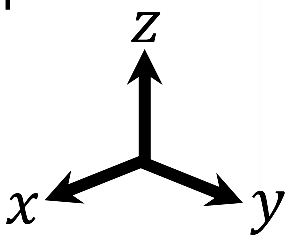

0.6% applied strain in build direction; periodic boundary conditions on sides of domain

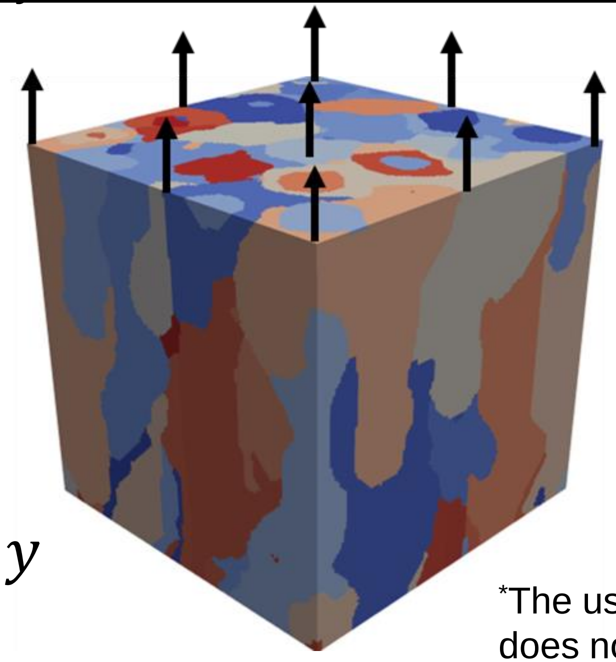

J.D. Pribe et al., 2023 [6]

*The use of specific software names does not imply an endorsement by the U.S. Government or NASA.

[7] R.A. Lebensohn et al., 2012

Structure-Property: Micromechanical Fields

- Goal: estimate distributions of fatigue indicator parameters (FIPs)

- Here: equivalent plastic strain

$$\varepsilon^p = \int \dot{\varepsilon}^p dt \qquad \dot{\varepsilon}^p = \sqrt{\frac{2}{3}\dot{\boldsymbol{\varepsilon}}^p : \dot{\boldsymbol{\varepsilon}}^p}$$

- Value assigned to each grain by volume averaging near hotspots

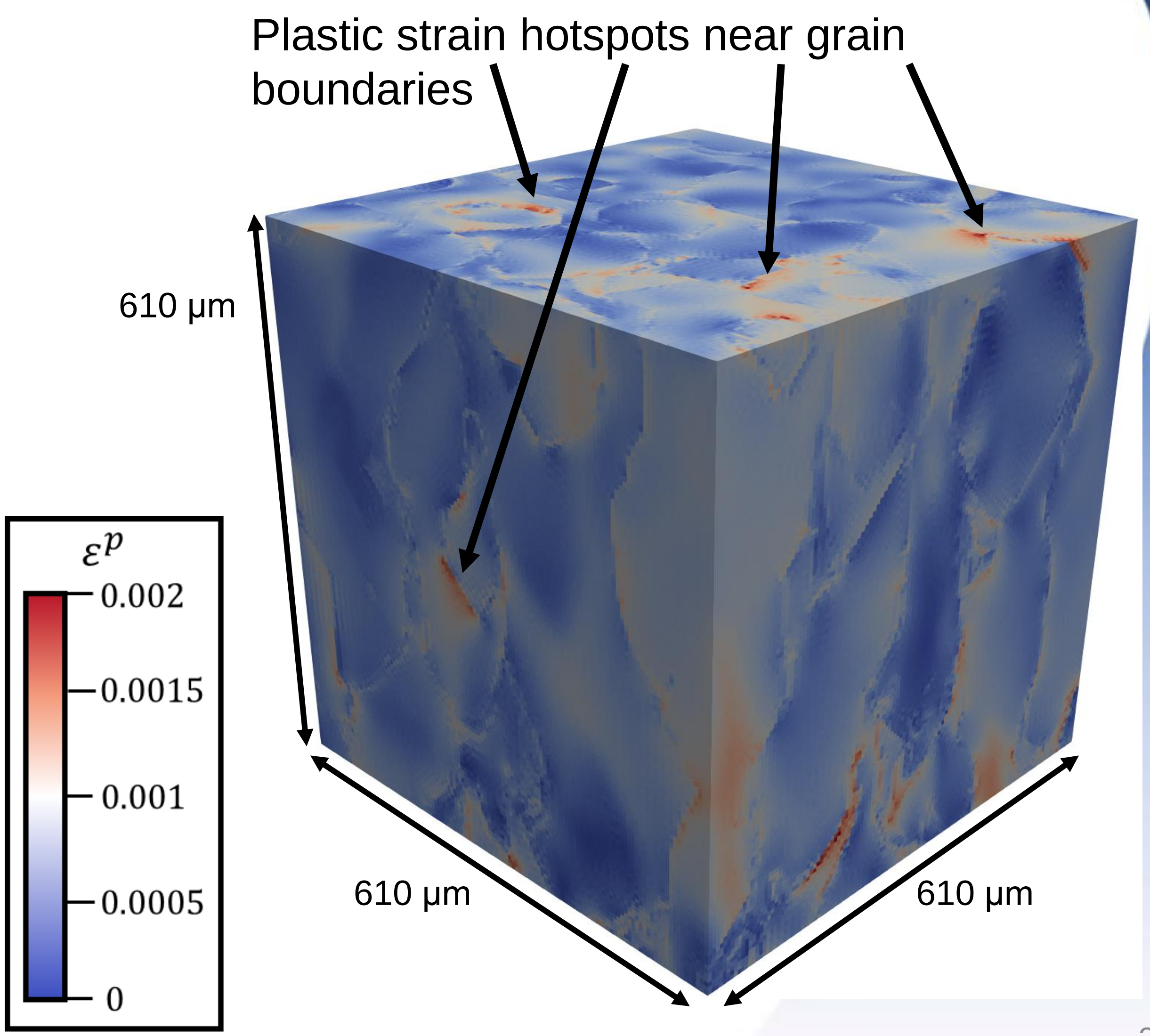

$\dot{\boldsymbol{\varepsilon}}^p$: plastic strain rate tensor

Microstructures with and without porosity

- Compare simulations with no porosity and with one 30-μm-diameter pore per simulation (~99.995% dense)
- Motivation: operating near the keyhole boundary could induce process-escape pores
  - Here: 370 W laser power, 1.2 m/s scan speed [8]; MAP estimates for thermophysical parameters

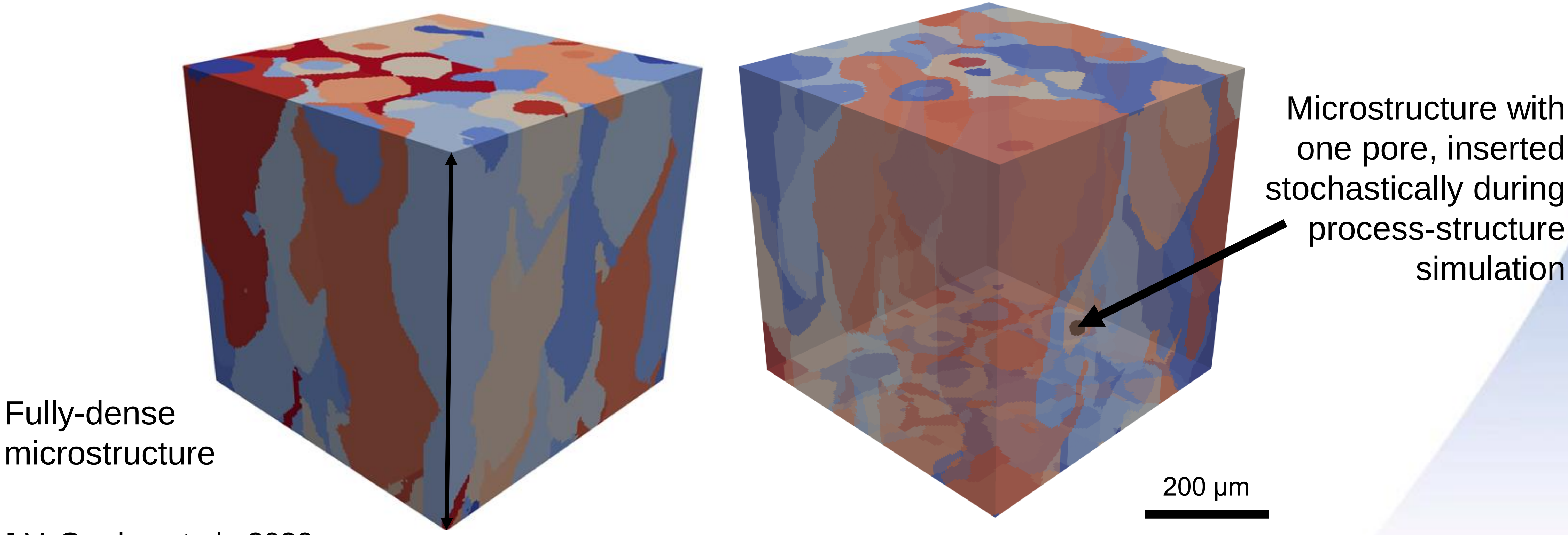

[8] J.V. Gordon et al., 2020

Microstructures with and without porosity

- 200 simulations with one 30-μm keyhole pore per simulation
- Overall distribution of plastic strain is similar
- But extreme values are shifted!

Example microstructure

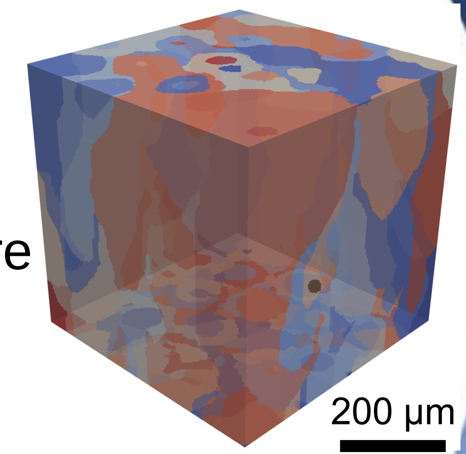

Equivalent plastic strain for all grains across 200 simulations

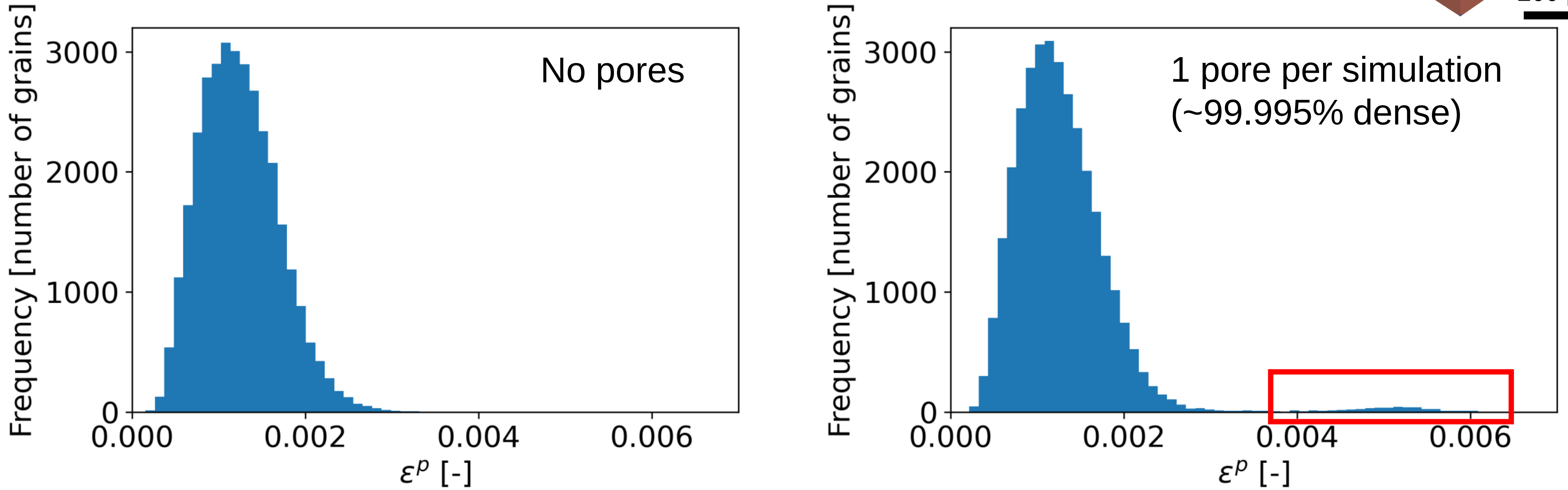

Microstructures with and without porosity

- 200 simulations with one 30-μm keyhole pore per simulation
- Overall distribution of plastic strain is similar
- But extreme values are shifted!
  - Bimodal distribution starts to develop

J.D. Pribe et al., 2023 [6]

Equivalent plastic strain for all grains across 200 simulations, log scale

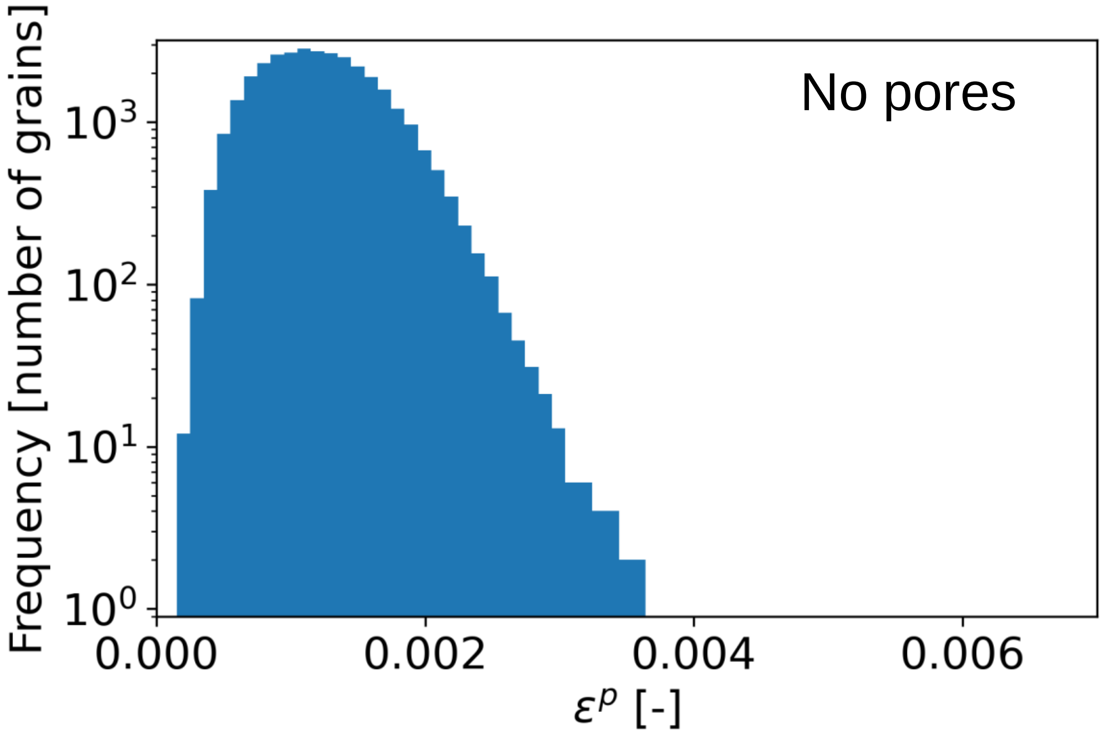

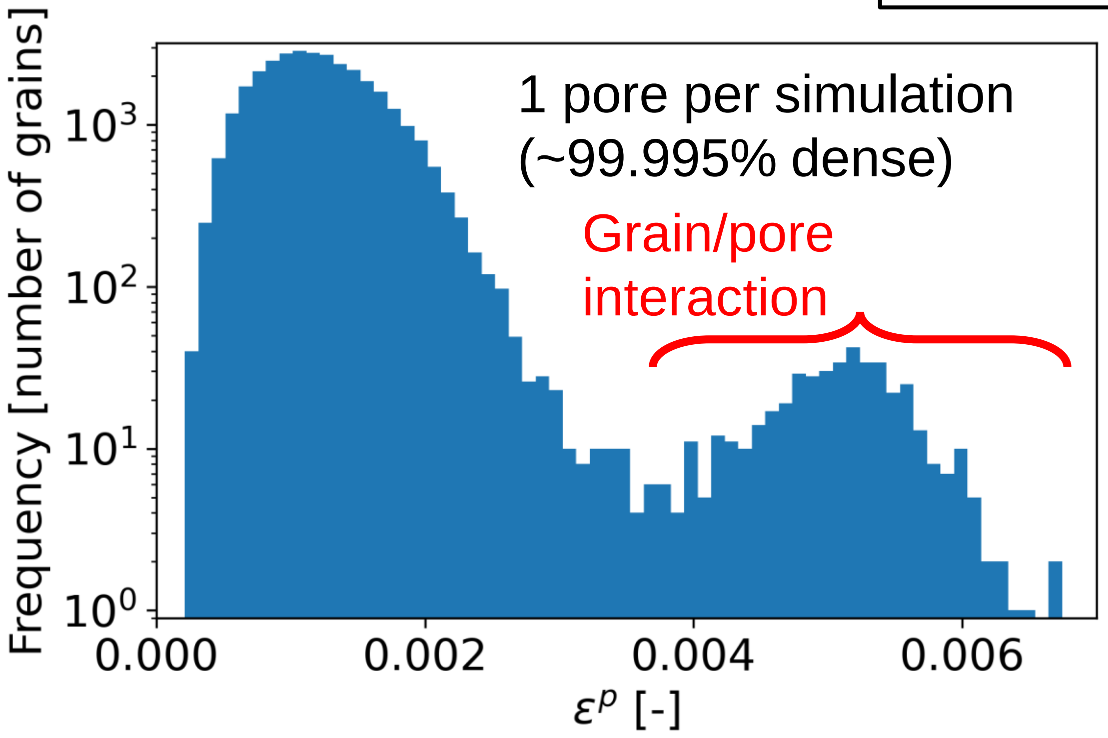

PSP Models: Revisiting Our Complete Approach

Melt Pool Modeling

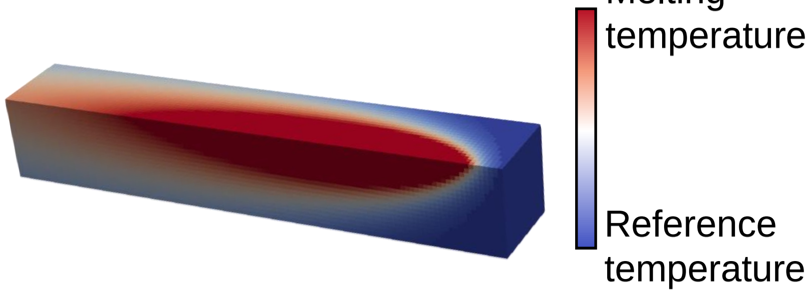

Process-Structure Models

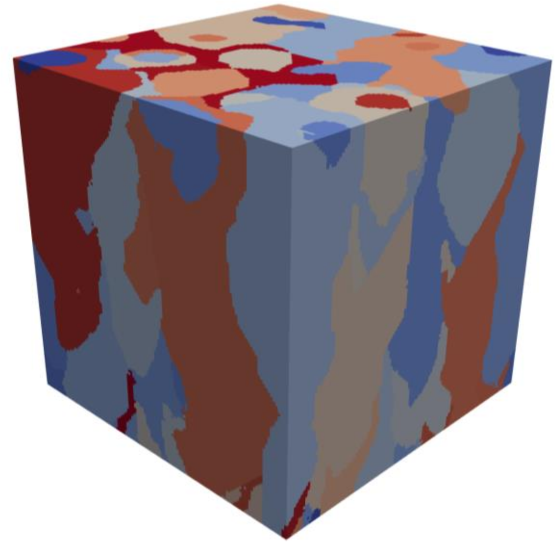

Defect Models

Keyhole porosity

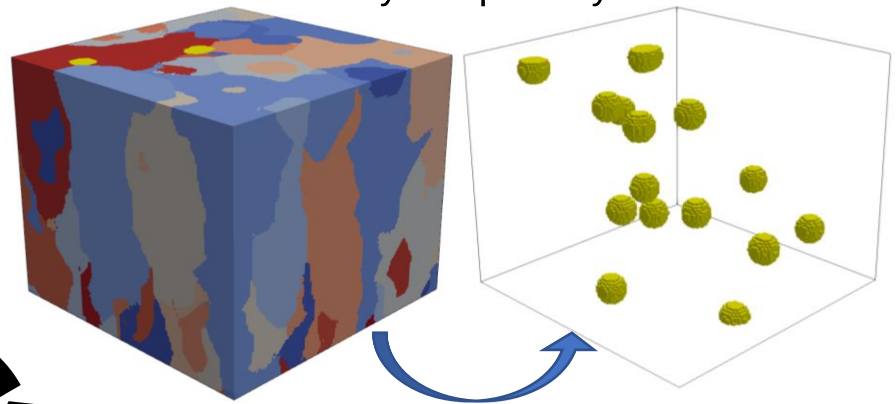

Lack-of-fusion
porosity

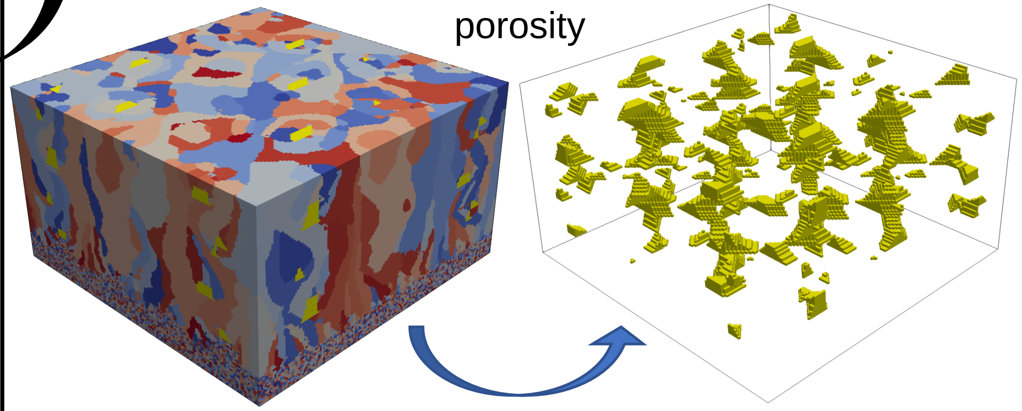

Structure-Property Models

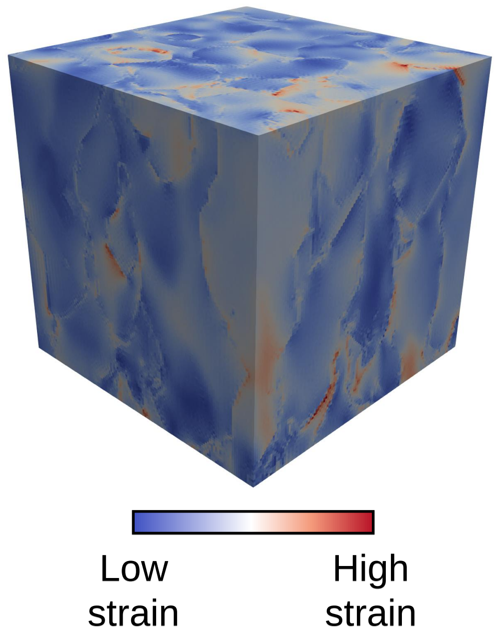

Targeted system size: >500 µm^3

Revisiting Initial Questions

What build parameters should I use? → Survey design space using PSP models

Should I be concerned about defects? → Apply defect models to predict if defects will occur

How will my new material perform? → Simulate performance using a Structure-Property model

Process-Structure-Property (PSP) models support solving these challenges

With continued maturity, it is hoped that PSP models will support next-generation, computational-materials augmented qualification and certification approaches

Acknowledgements and References

This work was supported by the NASA Aeronautics Research Mission Directorate (ARMD) Transformational Tools and Technologies (TTT) project, and the NASA Langley Research Center Internal Research and Development Program

[1] Rodgers, T.M. et al. "Simulation of powder bed metal additive manufacturing microstructures with coupled finite difference-Monte Carlo method," *Additive Manufacturing* 41 (2021): 101953
[2] Pauza, J.G. et al., "Computer simulation of microstructure development in powder-bed additive manufacturing with crystallographic texture." *Modelling and Simulation in Materials Science and Engineering* 29.5 (2021): 055019
[3] Richter, B. et al., “Integrated Monte Carlo microstructure and analytical temperature simulations of additive manufacturing,” Additive Manufacturing Benchmark 2022 Conference (2022), Bethesda, MD
[4] Gan, Z. et al., “Universal scaling laws of keyhole stability and porosity in 3D printing of metals,” *Nature Communications* 12.1 (2021): 2379
[5] Tang, M. et al., “Prediction of lack-of-fusion porosity for powder bed fusion,” Additive Manufacturing, 14 (2017): 39-48
[6] Pribe, J.D. et al., “A Process-Structure-Property Simulation Framework for Quantifying Uncertainty in Additive Manufacturing: Application to Fatigue in Ti-6Al-4V,” *Integrating Materials and Manufacturing Innovation* (2023): 1-20.
[7] Lebensohn, R.A. et al., “An elasto-viscoplastic formulation based on fast Fourier transforms for the prediction of micromechanical fields in polycrystalline materials,” *International Journal of Plasticity* 32.33 (2012): 59-69
[8] Gordon, J.V., “Defect structure process maps for laser powder bed fusion additive manufacturing,” *Additive Manufacturing* 36 (2020): 101552

Brodan Richter, brodan.m.richter@nasa.gov

Ed Glaessgen, e.h.glaessgen@nasa.gov

J.D. Pribe et al., 2023 [6]

Structure-property: Crystal plasticity

- **E**lasto-**V**isco**p**lastic **F**ast **F**ourier **T**ransform (EVP-FFT) [7]
- Advantages
  - Speed improvements over crystal plasticity finite element methods
  - Shares voxel-based microstructure representation with SPPARKS

Flow rule: $\dot{\boldsymbol{\varepsilon}}^p = \dot{\gamma}_0 \sum_{s=1}^{N_s} \boldsymbol{m}^s \left(\frac{|\boldsymbol{m}^s : \boldsymbol{\sigma}|}{\tau^s} \right)^n \operatorname{sgn}(\boldsymbol{m}^s : \boldsymbol{\sigma})$

Voce hardening: $\tau^s = \tau_0 + (\tau_1 + \theta_1 \Gamma) \left[1 - \exp\left(-\frac{\theta_0}{\tau_1} \Gamma \right) \right]$

$\Gamma = \sum_{s=1}^{N_s} \int \dot{\gamma}^s dt$

Implicit time discretization: $\boldsymbol{\sigma} = \mathbf{C} : \left(\boldsymbol{\varepsilon}_{t+\Delta t} - \boldsymbol{\varepsilon}_t^p - \dot{\boldsymbol{\varepsilon}}_{t+\Delta t}^p \Delta t \right)$

$\dot{\gamma}_0$: reference strain rate
n: viscoplastic exponent
$\dot{\boldsymbol{\varepsilon}}^p$: plastic strain rate tensor
$\boldsymbol{\sigma}$: stress tensor
$\boldsymbol{m}^s$: Schmid tensor for slip system *s*
τ^s: critical resolved shear stress for slip system *s*
$\dot{\gamma}^s$: plastic shear strain on slip system *s*
$\tau_0, \tau_1, \theta_0, \theta_1$: Voce hardening law parameters
Γ: accumulated slip on all slip systems
t, Δt: time, time step
$\mathbf{C}$: stiffness tensor
$\boldsymbol{\varepsilon}$: total strain tensor
$\boldsymbol{\varepsilon}^p$: plastic strain tensor

[7] R.A. Lebensohn et al., 2012

32

Structure-property: Validation

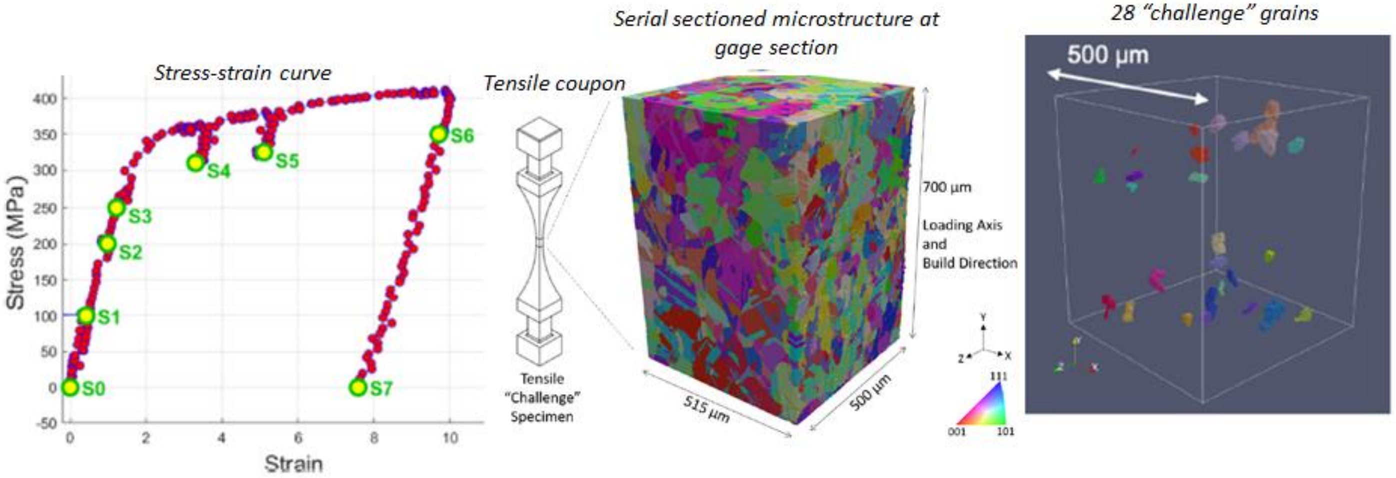

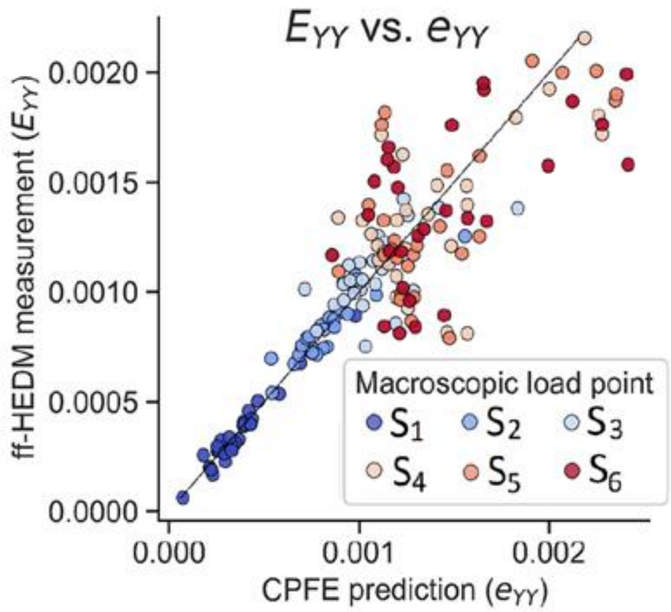

Challenge problem: Given the stress strain curve, serial-sectioned and reconstructed 3D microstructure, predict grain-average elastic strain tensor for 28 "challenge" grains at six different macroscopic load states, S1 through S6

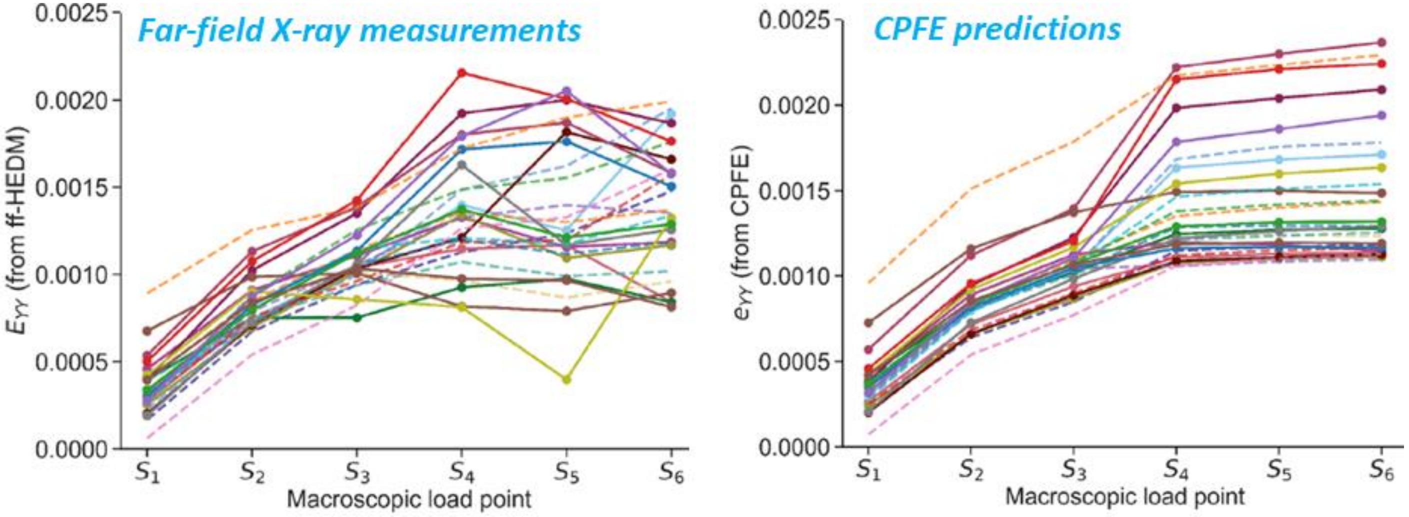

Yeratapally, S. et al., "*Effect of process-specific defects on the tensile and constant-amplitude fatigue behavior of as-built Ti-6Al-4V alloy produced by laser powder bed fusion process*", Additive Manufacturing Benchmarks (AM-Bench), August 15-18, 2022, Bethesda, Maryland.